

# On the Stability of Non-Extremal Conifold Backgrounds with Sources

---

Elena Cáceres<sup>a,b</sup> and Steve Young<sup>b</sup>

<sup>a</sup>*Facultad de Ciencias, Universidad de Colima, Mexico*

<sup>b</sup>*Theory Group, Department of Physics,  
University of Texas at Austin, Austin, TX 78727, USA.*

*E-mail:* [elenac@zippy.ph.utexas.edu](mailto:elenac@zippy.ph.utexas.edu), [scyoung@zippy.ph.utexas.edu](mailto:scyoung@zippy.ph.utexas.edu)

**ABSTRACT:** We present finite temperature solutions describing  $N_c$   $D5$  branes wrapped on the  $S^2$  of the resolved conifold in the presence of  $N_f$  flavor branes sources and their backreaction *i.e.*  $N_f/N_c \sim 1$ . In these solutions the dilaton does not blow up at infinity but stabilizes to a finite value. Thus, we can use them to generate new ones with  $D5$  and  $D3$  charge. The resulting backgrounds are non-extremal versions of the “flavored” resolved deformed conifold. It is tempting to interpret these solutions as gravity duals of finite temperature field theories exhibiting non-trivial phenomena as Seiberg dualities, Higgsing and confinement. However, a first necessary step in this direction is to investigate their stability. We study the specific heat of these new flavored backgrounds and find that they are thermodynamically unstable. Our results on the stability also apply to some of the non-extremal backgrounds with Klebanov-Strassler asymptotics found in the literature.

---

## Contents

<b>1</b>	<b>Introduction</b>	<b>2</b>
<b>2</b>	<b>Flavored backgrounds</b>	<b>3</b>
2.1	Review of flavored wrapped D5 backgrounds, $T = 0$	3
2.2	Non-extremal flavored backgrounds	6
<b>3</b>	<b>New non-extremal flavored solutions with stabilized dilaton</b>	<b>8</b>
3.1	UV expansions	9
3.2	IR asymptotics	10
3.3	Numerics	11
3.4	Temperature of the solutions	13
<b>4</b>	<b>Non-extremal backgrounds with flavored resolved deformed conifold asymptotics</b>	<b>14</b>
4.1	Equations of motion with $D3$ and $D5$ charges and smeared flavor branes	16
4.2	Rotating flavored non-extremal solutions	19
4.3	Asymptotics after the rotation	19
<b>5</b>	<b>Energy and specific heat</b>	<b>23</b>
<b>6</b>	<b>Conclusions</b>	<b>29</b>
<b>7</b>	<b>Acknowledgments</b>	<b>30</b>
<b>A</b>	<b>Appendix: U-Duality for the flavored, wrapped D5 branes black hole</b>	<b>30</b>
<b>B</b>	<b>Appendix: The equations of motion</b>	<b>33</b>
<b>C</b>	<b>Appendix: UV asymptotics</b>	<b>35</b>
C.1	Finite temperature UV asymptotics	35
C.2	Supersymmetric UV asymptotics	38
<b>D</b>	<b>Appendix: General form of <math>B_2</math></b>	<b>39</b>
<b>E</b>	<b>Appendix: Comments on numerical procedure</b>	<b>41</b>

---

# 1 Introduction

The gauge/gravity duality [1],[2],[3] provides a completely new framework for the understanding of strongly coupled field theories. It has opened a new area of study at the interface of field theory and string theory. The applications are numerous and include formal developments as well as phenomenological topics. One of the goals is to understand aspects of QCD, at zero and finite temperature, through the use of a suitable string dual. In this spirit, the two landmarks for non-conformal backgrounds with  $\mathcal{N} = 1$  supersymmetry — the deformed conifold model of Klebanov and Strassler [4] and the wrapped branes model of Maldacena and Núñez [5] — have been thoroughly studied and the connections between them well understood. In [6] it was shown that the Klebanov-Strassler background is a particular point in a one parameter family of IIB supergravity solutions. On the field theory side this family corresponds to different vacuum expectation values of a baryonic operator. Varying the string coupling constant of this family of SUGRA solutions smoothly interpolates between the Klebanov-Strassler and Maldacena-Núñez backgrounds. In order to incorporate dynamical flavor in the fundamental representation in these backgrounds we have to consider the backreaction of flavor branes. This difficult problem has been approached with a smearing technique that has been extensively used in the literature [7–12]. In particular, the backreaction of flavor  $D7$  branes in the Klebanov-Strassler was studied in [13],[14].

In [15] the authors presented a particular solution of wrapped  $D5$  branes that interpolates between the deformed conifold with flux and the resolved conifold with branes. Applying U-dualities to this solution adds  $D3$  charge and we recover the Klebanov-Strassler baryonic branch. The U-dualities do not rely on supersymmetry, and thus the same procedure can be applied to non-extremal backgrounds. This provides an alternative way of generating non-extremal deformations of KS. This method was used in [16] where finite temperature solutions with KS asymptotics were obtained. In this paper we present solutions that generalize the results of [16] in two ways: we consider the entire baryonic branch ( $a(r) \neq 0$ ) and we add flavor branes and their backreaction ( $s = N_f/N_c \sim \mathcal{O}(1)$ ).

As a prototype of a non-conformal theory, a finite temperature deformation of the KS baryonic branch could serve as a more realistic dual of finite temperature QCD. Examples of this type are notoriously difficult to find [17],[18] but it is undoubtedly a fascinating subject with rich new physics [19].

In [20] the authors obtained a flavored generalization of the KS baryonic branch. The dual field theory exhibits Seiberg dualities and Higgsing. This scenario was further developed in [21],[22],[23]. In the present work we construct finite temperature versions of [20] and study their stability. We consider non-extremal wrapped  $D5$ s that through

U-dualities result in a non-extremal deformation of the flavored deformed resolved conifold of [20]. As pointed out in [20], the backreaction of the flavorbranes modifies the asymptotics and the UV is KS only when the flavor is turned off,  $N_f \rightarrow 0$ . Thus, our solutions contain the finite-temperature backgrounds presented in [16] as a special case ( $N_f = 0$ ,  $a(r) = 0$ ).

We study the specific heat and show that it is negative and thus the backgrounds are unstable. These results apply also to the solutions of [24].

In the first sections of this paper we obtain non-extremal flavored solutions corresponding to fivebranes wrapped on the  $S^2$  of the resolved conifold. This will be the “seed” solution to which the solution generating technique will be applied. We present a general UV expansion that contains 11 parameters and determine the UV solution at any order. We then integrate back and match to the required regular horizon behavior. Once these solutions are under control we add  $D3$  charge through the U-dualities and arrive at a non-extremal flavored deformed resolved conifold. In section 5 we study the thermodynamic stability of the seed background (wrapped fivebranes) and of the background generated by U-duality. We find that they are both unstable. Our solutions contain as a special case the ones presented in [16] thus we expect our results to hold for those backgrounds as well.

## 2 Flavored backgrounds

### 2.1 Review of flavored wrapped D5 backgrounds, $T = 0$

In a seminal work, Casero, Nuñez and Paredes [25] presented a framework to incorporate the backreaction of the flavor D5-branes. The geometries obtained depend on the ratio  $N_f/N_c$  which can be of order one even in the  $N_c \rightarrow \infty$  limit. These spaces are singular at the origin, but the singularity is a “good” one in the sense of the criterion in [26] which means that the metric component  $g_{tt}$  remains finite in the limit  $r \rightarrow 0$ . Everywhere else the geometry is smooth and the curvature small as long as  $g_s N_c \gg 1$ . These backgrounds are conjectured to be dual to  $\mathcal{N} = 1$  SQCD in four dimensions with a large number of flavors, up to the same caveats concerning the decoupling of the KK modes that were already present in the discussion of the original Maldacena-Nuñez background without flavor.

The general strategy is the following [25]: One introduces a deformation of the Maldacena-Nuñez background due to the presence of flavor D5-branes, derives the corresponding BPS equations (see Appendix B of [25]), and attempts to solve them. The flavor D5-branes are taken to extend along the  $(x^0, x^1, x^2, x^3, \psi, r)$  directions and are smeared over the  $(\theta, \varphi, \tilde{\theta}, \tilde{\varphi})$  directions. These branes can be shown to preserve the same super-

symmetry as the background for arbitrary values of the angles  $\theta, \varphi, \tilde{\theta}, \tilde{\varphi}$  [27]. Moreover, the smeared flavor branes will be sources for the RR 3-form, resulting in RR fluxes in the deformed background that can be observed as a “violation” of the original Bianchi identity.

The ansatz for the deformation of the MN background ( $H_{(3)} = 0, F_{(5)} = 0$ ) is,

$$ds_{10}^2 = \alpha' g_s N_c e^{\phi(r)/2} \left[ \frac{1}{\alpha' g_s N_c} dx_{1,3}^2 + dr^2 + e^{2h(r)} (d\theta^2 + \sin^2 \theta d\varphi^2) + \frac{e^{2g(r)}}{4} ((w^1 + a(r)d\theta)^2 + (w^2 - a(r)\sin \theta d\varphi)^2) + \frac{e^{2k(r)}}{4} (w^3 + \cos \theta d\varphi)^2 \right], \quad (2.1)$$

The RR 3-form field strength reads

$$F_{(3)} = \frac{\alpha' g_s N_c}{4} \left[ -(w^1 + b(r)d\theta) \wedge (w^2 - b(r)\sin \theta d\varphi) \wedge (w^3 + \cos \theta d\varphi) + b' dr \wedge (-d\theta \wedge w^1 + \sin \theta d\varphi \wedge w^2) + (1 - b(r)^2) \sin \theta d\theta \wedge d\varphi \wedge w^3 \right], \quad (2.2)$$

and automatically satisfies the Bianchi identity  $dF_{(3)} = 0$ . The left-invariant one-forms  $\omega_a$  on  $S^3$  are

$$\begin{aligned} \omega_1 &= \cos \psi d\tilde{\theta} + \sin \psi \sin \tilde{\theta} d\tilde{\varphi}, \\ \omega_2 &= -\sin \psi d\tilde{\theta} + \cos \psi \sin \tilde{\theta} d\tilde{\varphi}, \\ \omega_3 &= d\psi + \cos \tilde{\theta} d\tilde{\varphi}. \end{aligned} \quad (2.3)$$

We also introduce the new radial coordinate  $\rho$ ,

$$d\rho = e^{-k(r)} dr, \quad (2.4)$$

and the standard notation

$$\begin{aligned} e_1 &= d\theta, \quad e_2 = \sin \theta d\varphi \\ \tilde{\omega}_1 &= \omega_1 + a(\rho)e_1, \quad \tilde{\omega}_2 = \omega_2 - a(\rho)e_2, \quad \tilde{\omega}_3 = \omega_3 + \cos \theta d\varphi. \end{aligned} \quad (2.5)$$

The metric then becomes

$$ds_{10}^2 = e^{\phi(\rho)/2} \left[ dx_{1,3}^2 + e^{2k(\rho)} d\rho^2 + e^{2h(\rho)} (e_1^2 + e_2^2) + \frac{e^{2g(\rho)}}{4} (\tilde{\omega}_1^2 + \tilde{\omega}_2^2) + \frac{e^{2k(\rho)}}{4} (\tilde{\omega}_3)^2 \right], \quad (2.6)$$

where we have set  $\alpha' g_s = 1$  and  $N_c$  has been absorbed into  $e^{2h}, e^{2g}, e^{2k}$  and  $d\rho^2$ . To be able to account for the backreaction of the flavor branes, the action must be augmented by the DBI and Wess-Zumino actions for the flavor D5-branes. The complete action then reads

$$S = S_{\text{grav}} + S_{\text{sources}}, \quad (2.7)$$

where, in Einstein frame, we have

$$S_{\text{grav}} = \frac{1}{2\kappa_{(10)}^2} \int d^{10}x \sqrt{-g_{(10)}} \left( R - \frac{1}{2}(\partial_\mu \phi)(\partial^\mu \phi) - \frac{1}{12}e^\phi F_{(3)}^2 \right), \quad (2.8)$$

and

$$S_{\text{sources}} = T_5 \sum_{N_f} \left( - \int_{\mathcal{M}_6} d^6x e^{\phi/2} \sqrt{-g_{(6)}} + \int_{\mathcal{M}_6} P[C_{(6)}] \right). \quad (2.9)$$

One of the effects of smearing the  $N_f \rightarrow \infty$  flavor branes along the two transverse 2-spheres is that there will be no dependence on the angular coordinates  $(\theta, \varphi, \tilde{\theta}, \tilde{\varphi})$  of the functions  $f(\rho), h(\rho), g(\rho)$  and  $k(\rho)$  that determine our metric ansatz (2.6) — significantly simplifying the computations. After the smearing we can write

$$S_{\text{sources}} = \frac{T_5 N_f}{(4\pi)^2} \left( - \int d^{10}x \sin \theta \sin \tilde{\theta} e^{\phi/2} \sqrt{-g_{(6)}} + \int \text{Vol}(\mathcal{Y}_4) \wedge C_{(6)} \right), \quad (2.10)$$

with the definition  $\text{Vol}(\mathcal{Y}_4) = \sin \theta \sin \tilde{\theta} d\theta \wedge d\varphi \wedge d\tilde{\theta} \wedge d\tilde{\varphi}$ . Once the smeared flavor D5-branes are incorporated into the background, the Bianchi identity for  $F_{(3)}$  (which is identical to the EOM for  $C_{(6)}$ ) gets modified to

$$dF_{(3)} = \frac{N_f}{4} \sin \theta \sin \tilde{\theta} d\theta \wedge d\varphi \wedge d\tilde{\theta} \wedge d\tilde{\varphi} = \frac{N_f}{4} \omega_1 \wedge \omega_2 \wedge e_1 \wedge e_2. \quad (2.11)$$

as a result of adding a Wess-Zumino term. This can be solved by adding the following term to the original  $F_{(3)}$  in (2.2),

$$F_{(3)}^{\text{sources}} = -\frac{N_f}{4} e_1 \wedge e_2 \wedge \omega_3 \quad (2.12)$$

The full RR 3-form field strength now reads

$$\begin{aligned} F_{(3)} = \frac{N_c}{4} \left[ -(\omega_1 + b e_1) \wedge (\omega_2 - b e_2) \wedge \tilde{\omega}_3 \right. \\ \left. + b' d\rho \wedge (-e_1 \wedge \omega_1 + e_2 \wedge \omega_2) + \left( 1 - b^2 - \frac{N_f}{N_c} \right) e_1 \wedge e_2 \wedge \omega_3 \right] \equiv \frac{\alpha' N_c}{4} f_3, \end{aligned} \quad (2.13)$$

where the only modification is the appearance of the term involving  $N_f/N_c$  in the second line.

The first order BPS equations for this ansatz can be solved for  $b(\rho), h(\rho), g(\rho)$  leaving a system of three coupled differential equations for  $a(\rho), k(\rho)$  and  $\phi(\rho)$ . The details can be found in [25, 28, 29]. In the present work we will be interested in non-extremal generalizations of these flavored backgrounds. The non-zero temperature breaks supersymmetry and thus we cannot resort to the BPS equations nor to the master equation formalism developed in [28]. We are bound to solve the second order equations of motion (EOMs) obtained from the action (2.8 - 2.9).

## 2.2 Non-extremal flavored backgrounds

One of our goals is to find non-extremal deformations of the flavored backgrounds presented in the previous section. To that aim we consider the following ansatz for the metric,

$$\begin{aligned} ds_{IIB}^2 = & e^{\phi/2} \left[ -e^{-8x} dt^2 + dx_1^2 + dx_2^2 + dx_3^2 \right] + e^{\phi/2} ds_6^2, \\ ds_6^2 = & \left[ e^{8x} e^{2k} d\rho^2 + \frac{e^{2k}}{4} (\omega_3 + \cos \theta d\varphi)^2 + e^{2h} (d\theta^2 + \sin^2 \theta d\varphi^2) \right. \\ & \left. + \frac{e^{2g}}{4} ((\omega_1 + a(\rho) d\theta)^2 + (\omega_2 - a(\rho) \sin \theta d\varphi)^2) \right] \end{aligned} \quad (2.14)$$

and the RR 3-form gauge field

$$F_{(3)} = \frac{N_c}{4} f_3 \quad (2.15)$$

where  $f_3$  is defined in (2.13).

This ansatz is general enough to account for the effect of the backreaction of a large number  $N_f$  of flavor D5 branes, smeared along the  $\theta, \varphi, \tilde{\theta}, \tilde{\varphi}$  directions, and spanning both the Minkowski and  $\rho$  directions. This gives a source contribution to the  $F_3$  Bianchi identity, which we define as the smearing form  $\Xi_{(4)}$ :

$$\Xi_{(4)} \equiv dF_3 = \frac{N_f}{4} \omega_1 \wedge \omega_2 \wedge e_1 \wedge e_2. \quad (2.16)$$

The factor  $e^{8x(\rho)}$  is a non-extremal deformation that accounts for the appearance of a horizon. The total Lagrangian for the bulk fields and smeared flavor branes is

$$S = S_{\text{grav}} + S_{\text{sources}}, \quad (2.17)$$

where  $S_{\text{grav}}$  and  $S_{\text{sources}}$  are given in (2.8) and (2.10) respectively.

Introducing the ansatz (2.14 - 2.15) in the action and integrating over the angular variables, we are left with a one dimensional Lagrangian from which we can derive the EOMs for all the fields. We obtain<sup>1</sup>,

$$\begin{aligned}
& -\frac{1}{8}e^{-4h+8x}s^2 + \frac{1}{4}e^{-2g-4h+8x}s \left( -2e^{2(h+k)} + e^{2g}(1-2ba+a^2) \right) \\
& + \frac{1}{8}e^{-4(g+h)} \left( -16e^{4h+8x} - e^{4g+8x}(1-2ba+a^2)^2 + 2e^{2(g+h)}(-4e^{8x}(b-a)^2 - b'^2) \right) \\
& + 2(g' + h' - 4x')\Phi' + 2\Phi'^2 + \Phi'' = 0
\end{aligned} \tag{2.18}$$

$$2g'x' + 2h'x' - 8x'^2 + 2x'\Phi' + x'' = 0 \tag{2.19}$$

$$\begin{aligned}
& \frac{1}{8}e^{-4(g+h-2x)} \left[ e^{4g} + 16e^{4h} - e^{4(g+k)} - 16e^{4(h+k)} - 2e^{4g}s + e^{4g}s^2 \right. \\
& + 2e^{2g}(4e^{2h} + 4e^{4g+2h} + e^{2g+4k} - 4e^{2h+4k} - e^{2g}(-1+s))a^2 - e^{4g}(-1+e^{4k})a^4 \\
& \left. - 4e^{2g}ba(4e^{2h} - e^{2g}(-1+s) + e^{2g}a^2) + b^2(8e^{2(g+h)} + 4e^{4g}a^2) \right] \\
& + 2k'(g' + h' - 4x' + \Phi') + k'' = 0
\end{aligned} \tag{2.20}$$

$$\begin{aligned}
& \frac{1}{8}e^{-2(g+2h)} \left[ -8e^{2(g+h+k+4x)} + e^{2g+8x} + e^{2g+4k+8x} + 4e^{2(h+k+4x)}s - 2e^{2g+8x}s \right. \\
& + e^{2g+8x}s^2 + 2e^{8x}(2e^{2h} + 2e^{4g+2h} - 4e^{2(g+h+k)} - e^{2g+4k} + 2e^{2h+4k} - e^{2g}(-1+s))a^2 \\
& + e^{2g+8x}(1+e^{4k})a^4 + 4e^{8x}b^2(e^{2h} + e^{2g}a^2) - 4e^{8x}ba(2e^{2h} - e^{2g}(-1+s) + e^{2g}a^2) \\
& \left. + e^{2h}b'^2 + e^{4g+2h}a'^2 \right] + 2h'(g' - 4x' + \Phi') + 2h'^2 + h'' = 0
\end{aligned} \tag{2.21}$$

$$\begin{aligned}
& \frac{1}{8}e^{-2(2g+h)} \left[ -32e^{2(g+h+k+4x)} + 16e^{2h+8x} + 16e^{2h+4k+8x} + 4e^{2(g+k+4x)}s \right. \\
& + 4e^{2g+8x}b^2 - 8e^{2g+8x}ba - 4e^{2g+8x}(-1+e^{4g}-e^{4k})a^2 + e^{2g}b'^2 - e^{6g}a'^2 \left. \right] \\
& + 2g'(h' - 4x' + \Phi') + 2g'^2 + g'' = 0
\end{aligned} \tag{2.22}$$

$$\begin{aligned}
& e^{-4g-2h+8x} \left[ -2e^{2g}b^2a + b(4e^{2h} - e^{2g}(-1+s) + 3e^{2g}a^2) \right. \\
& \left. - a(4e^{2h}(1+e^{4g}+e^{4k}) - 8e^{2(g+h+k)} - e^{2g+4k} - e^{2g}(-1+s) + e^{2g}(1+e^{4k})a^2) \right] \\
& + 2a'(2g' - 4x' + \Phi') + a'' = 0
\end{aligned} \tag{2.23}$$

---

<sup>1</sup>We set  $\alpha' = g_s = 1$ , therefore  $T_5 = \frac{1}{(2\pi)^5}$  and  $2\kappa_{(10)}^2 = (2\pi)^7$ .



$$-4e^{8x}b + 4e^{8x}a + e^{2g-2h+8x}a(1-s-2ba+a^2) + b'(-8x' + 2\Phi') + b'' = 0. \quad (2.24)$$

These equations should be solved together with the constraint coming from reparametrization invariance,

$$\begin{aligned} & \frac{1}{256}e^{-4(g+h)} \left[ (-e^{4(g+k+2x)} - 16e^{4(h+k+2x)} + 16e^{2(2g+h+k+4x)} + 64e^{2(g+2h+k+4x)} \right. \\ & - e^{4g+8x} - 16e^{4h+8x} - 8e^{2(g+h+k+4x)}s + 2e^{4g+8x}s - e^{4g+8x}s^2 \\ & - 2e^{2g+8x}(4e^{2h} + 4e^{4g+2h} - 8e^{2(g+h+k)} - e^{2g+4k} + 4e^{2h+4k} - e^{2g}(-1+s))a^2 \\ & - e^{4g+8x}(1+e^{4k})a^4 + 4e^{2g+8x}a(4e^{2h} - e^{2g}(-1+s) + e^{2g}a^2)b \\ & \left. - 4e^{2g+8x}(2e^{2h} + e^{2g}a^2)b^2 + 2e^{6g+2h}a'^2 + 2e^{2(g+h)}b'^2 \right] \\ & - \frac{1}{16}(g'^2 + h'^2 + 2h'(k' - 4x') + 2g'(2h' + k' - 4x') - 4k'x') \\ & + \frac{1}{8}(-2g' - 2h' - k' + 4x')\Phi' - \frac{1}{8}\Phi'^2 = 0 \end{aligned} \quad (2.25)$$

The details of the derivation are given in Appendix B.

### 3 New non-extremal flavored solutions with stabilized dilaton

In this section, we numerically solve the Einstein equations of motion (2.18)-(2.25). Our method combines the virtues of the approaches developed in [17] and [18, 30]. Following [17] we first find a set of parameters that completely determines the UV behavior of the solutions to any order. In our case there turn out to be eleven free parameters. The IR behavior is determined by regularity at the horizon and involves seven free parameters. We then solve numerically the equations of motion and the constraint using these expansions as boundary conditions. To derive the EOMs we follow the framework in [31] (see Appendix B for details).

Two points are worth mentioning

- The solutions we are looking for are non-extremal deformations of the supersymmetric flavored solutions studied in [20]; thus we choose certain UV parameters so that the UV asymptotics reduce to the supersymmetric solutions when a parameter related to the temperature goes to zero.

- An important feature of our solutions is a dilaton whose value is “stabilized” — *i.e.* it asymptotes to a constant value in the UV. This property is required if the rotation procedure is to produce new solutions where the gravity modes decouple.

### 3.1 UV expansions

To determine the UV behavior of the metric and gauge functions for a finite-temperature deformation of the flavored solutions of [20], we begin by taking a UV series expansion of the form

$$\begin{aligned}
e^{2h} &= \sum_{i=0}^{\infty} \sum_{j=0}^i h_{i,j} \rho^j e^{4(1-i)\rho/3} & e^{4\phi} &= \sum_{i=1}^{\infty} \sum_{j=0}^i f_{i,j} \rho^j e^{4(1-i)\rho/3} \\
e^{2g} &= \sum_{i=0}^{\infty} \sum_{j=0}^i g_{i,j} \rho^j e^{4(1-i)\rho/3} & e^{8x} &= \sum_{i=1}^{\infty} \sum_{j=0}^i x_{i,j} \rho^j e^{2(1-i)\rho/3} \\
e^{2k} &= \sum_{i=0}^{\infty} \sum_{j=0}^i k_{i,j} \rho^j e^{4(1-i)\rho/3} & a &= \sum_{i=1}^{\infty} \sum_{j=0}^i a_{i,j} \rho^j e^{2(1-i)\rho/3} \\
&& b &= \sum_{i=1}^{\infty} \sum_{j=0}^i b_{i,j} \rho^j e^{2(1-i)\rho/3}, \quad (3.1)
\end{aligned}$$

and requiring that it satisfies the Einstein equations given in Appendix B. For an expansion of this form, we find that all of the coefficients — up to arbitrary order — are determined in terms of a set of eleven free parameters. Details of the relations between the expansion coefficients are given in Appendix C.1. We next set a number of the free parameters to agree with the supersymmetric UV asymptotics of [20] (summarized in Appendix C.2):

$$\begin{aligned}
f_{1,0} &= 1, \quad f_{3,0} = 3/4c_+^2 - 3s/4c_+^2 + 51s^2/8c_+^2, \quad h_{1,0} = -1/4 + 13s/32, \\
k_{0,0} &= 2c_+/3, \quad k_{3,0} = \frac{-512c_+^3 + 8c_- + 3s(32 - 32s + 17s^2)}{384c_+^2}, \quad h_{1,1} = 1/2 - s/4, \\
a_{2,0} &= 0, \quad a_{4,0} = 2, \quad b_{4,0} = 0 \quad (3.2)
\end{aligned}$$

After doing this, the asymptotics reduce to those of [20] in the limit where the parameter  $x_{5,0}$  goes to zero. In order to agree with the convention used in [16], we will refer to the parameter  $x_{5,0}$  as  $C_2$  in what follows.<sup>2</sup> With the choice of parameters in

---

<sup>2</sup>Note however, that the sign of our  $C_2$  is flipped with respect to theirs: we expand  $e^{8x}$ , whereas they expand  $e^{-8x}$ .

equation (3.2), the UV asymptotics of our metric and gauge functions are given by

$$\begin{aligned}
e^{8x} &= 1 + C_2 e^{-8\rho/3} - \frac{C_2 e^{-4\rho} s}{2c_+} + \mathcal{O}(e^{-8\rho/3}) \\
e^{2k} &= \frac{2}{3} c_+ e^{4\rho/3} + \frac{s}{2} - \frac{e^{-4\rho/3} (400 - 400s + 91s^2 - 160(-2+s)^2 \rho + 64(-2+s)^2 \rho^2)}{96c_+} + \mathcal{O}(e^{-8\rho/3}) \\
e^{2h} &= \frac{1}{4} c_+ e^{4\rho/3} + \frac{1}{32} (-8 + 13s - 8(-2+s)\rho) \\
&\quad + \frac{1}{256c_+} e^{-4\rho/3} (208 - 208s + 43s^2 - 64(-2+s)^2 \rho + 64(-2+s)^2 \rho^2) + \mathcal{O}(e^{-8\rho/3}) \\
e^{2g} &= c_+ e^{4\rho/3} + \left(1 + \frac{5s}{8}\right) + (-2+s)\rho \\
&\quad + \frac{1}{64c_+} e^{-4\rho/3} (208 - 208s + 43s^2 - 64(-2+s)^2 \rho + 64(-2+s)^2 \rho^2) + \mathcal{O}(e^{-8\rho/3}) \\
e^{4\phi} &= 1 - \frac{3e^{-4\rho/3} s}{c_+} + \frac{e^{-8\rho/3} (6 + s^2(51 - 12t) - 48t + 6s(-1 + 8t))}{8c_+^2} + \mathcal{O}(e^{-4\rho}) \\
a &= 2e^{-2\rho} + \mathcal{O}(e^{-10\rho/3}) \quad b = 2e^{-2\rho} (2 - s)\rho + \mathcal{O}(e^{-14\rho/3}). \tag{3.3}
\end{aligned}$$

All of these expressions in fact depend on  $C_2$ , but only at higher order than we have shown here. The parameter  $c_-$  also enters at higher order. In our numerical solutions, we will set  $c_-$  equal to 0 for simplicity. This choice of UV behavior leaves us with three free parameters:  $c_+$ ,  $C_2$ , and  $s$ .

### 3.2 IR asymptotics

Near the horizon,  $\rho = \rho_h$ , we expand the equations of motion in a power series up to fifth order:<sup>3</sup>

$$\begin{aligned}
e^{-8x(\rho)} &= x_1(\rho - \rho_h) + x_2(\rho - \rho_h)^2 + x_3(\rho - \rho_h)^3 + x_4(\rho - \rho_h)^4 + x_5(\rho - \rho_h)^5 + \dots \\
e^{2h(\rho)} &= h_0 + h_1(\rho - \rho_h) + h_2(\rho - \rho_h)^2 + h_3(\rho - \rho_h)^3 + h_4(\rho - \rho_h)^4 + h_5(\rho - \rho_h)^5 + \dots \\
&\dots \\
\Phi(\rho) &= f_0 + f_1(\rho - \rho_h) + f_2(\rho - \rho_h)^2 + f_3(\rho - \rho_h)^3 + f_4(\rho - \rho_h)^4 + f_5(\rho - \rho_h)^5 + \dots \\
a(\rho) &= a_0 + a_1(\rho - \rho_h) + a_2(\rho - \rho_h)^2 + a_3(\rho - \rho_h)^3 + a_4(\rho - \rho_h)^4 + a_5(\rho - \rho_h)^5 + \dots \\
b(\rho) &= b_0 + b_1(\rho - \rho_h) + b_2(\rho - \rho_h)^2 + b_3(\rho - \rho_h)^3 + b_4(\rho - \rho_h)^4 + b_5(\rho - \rho_h)^5 + \dots \tag{3.4}
\end{aligned}$$

---

<sup>3</sup>The horizon expansion could be taken to higher order to improve accuracy. However, due to the presence of  $s$  the expressions grow unwieldy in complexity. We find that a fifth order expansion provides enough accuracy to obtain well behaved numerical solutions.

Demanding that these expansions satisfy the equations of motion, we derive expressions for  $x_2, \dots, h_1, \dots, g_1, \dots, k_1, \dots, f_1, \dots, a_1, \dots, b_1, \dots$  in terms of  $x_1, h_0, g_0, k_0, a_0, b_0$ .<sup>4</sup> Along with  $f_0$ , this gives seven independent parameters coming from the horizon expansion. The expressions for the dependent coefficients are quite cumbersome and we will not present their explicit form here; a Mathematica file is available from the authors upon request.

### 3.3 Numerics

In this section we outline the numerical procedure used to find solutions to the equations of motion (2.18)-(2.24) that have a horizon at finite  $\rho = \rho_h$  and obey boundary conditions (3.3). Due to the large dimensional parameter space (3 free parameters in the UV and 7 in the IR) this is a difficult numerical problem. The numerical method we use does not pretend to solve the problem in all generality and is not a tool to thoroughly study the full parameter space. However, within certain limitations to be elucidated below, it allows us to construct numerical solutions with enough accuracy to determine the temperature, energy and specific heat of these backgrounds. More details of the numerics are given in Appendix E.

Our strategy is to start in the UV where there are fewer free parameters. We pick a set of values for  $c_+$  and  $C_2$ ,<sup>5</sup> which determine the UV behavior of the background.

With these UV boundary conditions, we integrate back from  $\rho_\infty$  and look for values of  $c_+$  and  $C_2$  which produce solutions with horizon behavior. We will refer to these solutions as the *UV-shot* solutions. The value of  $\rho_\infty$  is chosen such that the dilaton reaches its asymptotic value,  $e^{4\phi}|_{\rho_\infty} \sim 1$ . We next require that this numerical solution matches the horizon expansion (3.4) and its derivatives up to fifth order. Doing this for a given choice of  $(c_+, C_2)$  determines the free parameters  $(x_1, h_0, g_0, k_0, f_0, a_0, b_0)$ . A black hole solution will not exist for every choice of  $(c_+, C_2)$ ; for some values of  $(c, C_2)$  there will not be a horizon and for others there may be naked singularities outside the horizon.

In order to match the solution to the horizon expansion, we define a “mismatch” function evaluated at a point  $\rho_0$  close to the horizon,  $\rho_0 = \rho_h + \epsilon$ .

$$\begin{aligned} m(\rho_0) = & [x_{sh}(\rho_0) - x_{num}(\rho_0)]^2 + [x'_{sh}(\rho_0) - x'_{num}(\rho_0)]^2 + [g_{sh}(\rho_0) - g_{num}(\rho_0)]^2 + \\ & [g'_{sh}(\rho_0) - g'_{num}(\rho_0)]^2 + [h_{sh}(\rho_0) - h_{num}(\rho_0)]^2 + [h'_{sh}(\rho_0) - h'_{num}(\rho_0)]^2 + \\ & [k_{sh}(\rho_0) - k_{num}(\rho_0)]^2 + [k'_{sh}(\rho_0) - k'_{num}(\rho_0)]^2 \end{aligned} \quad (3.5)$$

The subscript *num* denotes the UV-shot numerical solution and *sh* denotes the series expansion (3.4). In [16] the authors used a similar technique to find abelian,  $a =$

---

<sup>4</sup>The higher order coefficients do not depend on  $f_0$ . This corresponds to the invariance of the EOMs under constant shifts in the dilaton.

<sup>5</sup>For simplicity, we set  $c_-$  equal to zero.

$b = 0$ , solutions. Unlike [16], here we are dealing with non-abelian solutions and due to numerical inaccuracies near the horizon, including  $a$ ,  $b$ , and  $\Phi$  in the mismatch function does not allow for an accurate matching. Our strategy to find the horizon parameters will be a three step procedure. First we will minimize a mismatch function  $m$  (that does not contain  $a$ ,  $b$ , and  $\Phi$ ) and determine  $(x_1, h_0, g_0, k_0)$ . Then we will tune  $a_0$  and  $b_0$  to eliminate unwanted behavior in  $b$ . Finally, we will use the invariance of the EOMs under constant shifts of the dilaton to set  $f_0$  so that the horizon-shot and UV-shot dilaton agree at the UV boundary. Keep in mind that we want to perform the matching as close to the horizon as possible and obtain stable solutions. We use the word “stable” loosely to mean horizon shot solutions that agree with the UV shot ones. This is not an easy task because close to the horizon the UV-shot solutions always display numerical inaccuracies. To overcome this problem we do the following: we first match at a larger value of  $\epsilon = 0.7$ , then we use the resulting values of the matched horizon parameters as seeds for a new match performed at a lower  $\epsilon = .15$ . In the last step we also constrain the allowed variance of  $(x_1, g_0, h_0, k_0)$  around the seed values until the resulting  $\epsilon = .15$  match gives horizon shot solutions which agree with the UV shot solutions. The end result is  $m(\rho_h + .15) < 10^{-7}$  and a set of parameters highly tuned to give stable solutions.

With these parameters we shoot from the horizon and show that our solutions also satisfy the constraint coming from reparametrization invariance,  $T + U = 0$ . We use `WorkingPrecision` = 40 and obtain solutions that satisfy  $T + U < \sim 10^{-6}$  throughout the interval. Figs.(1 - 4) show two solutions for different  $(c_+, C_2)$  values.

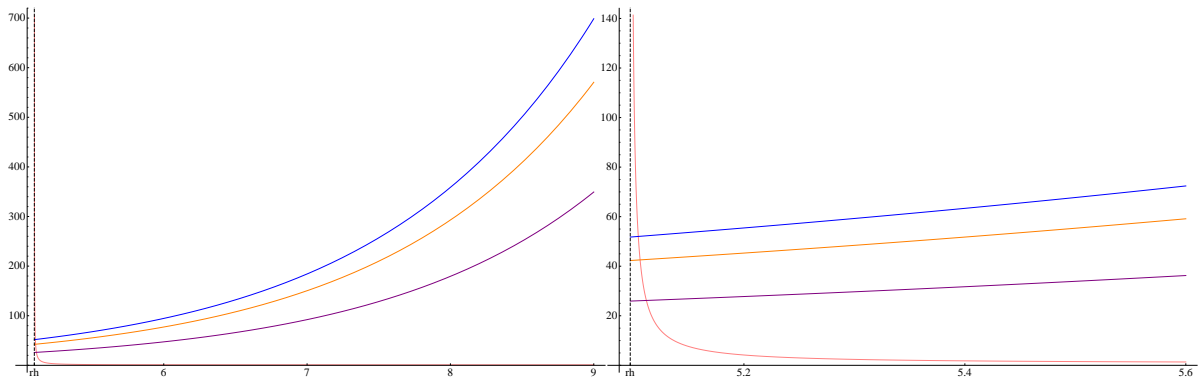


**Figure 1.** Horizon-shot and UV-shot solutions for metric functions at  $s = 1$ ,  $c_+ = 3$ ,  $C_2 = 800000$ .  $e^k$  - orange,  $e^g$  - blue,  $e^h$  - purple,  $e^{8x}$  - pink

**Figure 2.** Horizon-shot and UV-shot solutions for metric functions at  $s = 1$ ,  $c_+ = 3$ ,  $C_2 = 800000$ . Zoomed into region near horizon at  $\rho_h \sim 5.097$ .

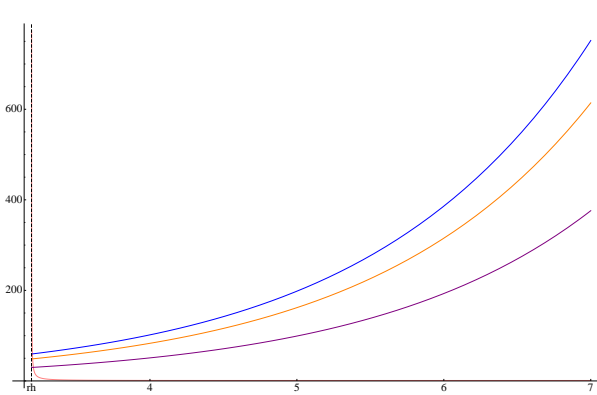


**Figure 3.** Horizon-shot and UV-shot solutions for metric functions at  $s = 1$ ,  $c_+ = 50$ ,  $C_2 = 5000$ .

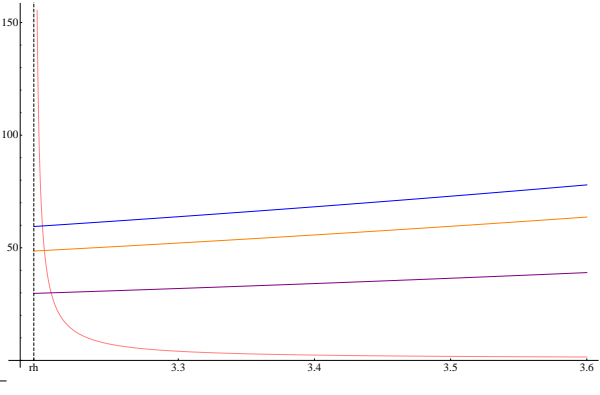


**Figure 4.** Horizon-shot and UV-shot solutions for metric functions at  $s = 1$ ,  $c_+ = 50$ ,  $C_2 = 5000$ . Zoomed into region near horizon at  $\rho_h \sim 3.19$

### 3.4 Temperature of the solutions

The expression for the horizon temperature of our solutions follows from the standard prescription of analytically continuing the solution to Euclidean time and imposing the periodicity of this coordinate. The temperature is then given by  $T = 1/\beta$ , where the period  $\beta$  is determined by requiring the regularity of the Euclideanized metric at the horizon. We use the numerically determined parameters described in section 3.2 to describe the metric at the horizon; of these parameters, only  $x_1$  and  $k_0$  enter into the expression for the temperature, which is found to be

$$T_{hor} = \frac{1}{4\pi} \frac{x_1}{\sqrt{k_0}}. \quad (3.6)$$

In [16] it was shown that the horizon temperature is the same for pre- and post-rotated solutions. It can be checked that this is still the case here. In Figs.(5) and (6) we see that the horizon temperature has negligible dependence on  $N_f/N_c$  for fixed values of  $c_+$  and  $C_2$ . In Figs.(7) and (8) we show how the horizon temperature varies with  $C_2$  for fixed values of  $c_+$  and  $s$ .

The dependence of the horizon temperature on the amount of flavor added is minor compared to its dependence on  $C_2$ . For a fixed  $c_+$  value, the change in a plot like Fig.(7) as we vary  $0 \leq s < \sim 10$  is almost unnoticeable.

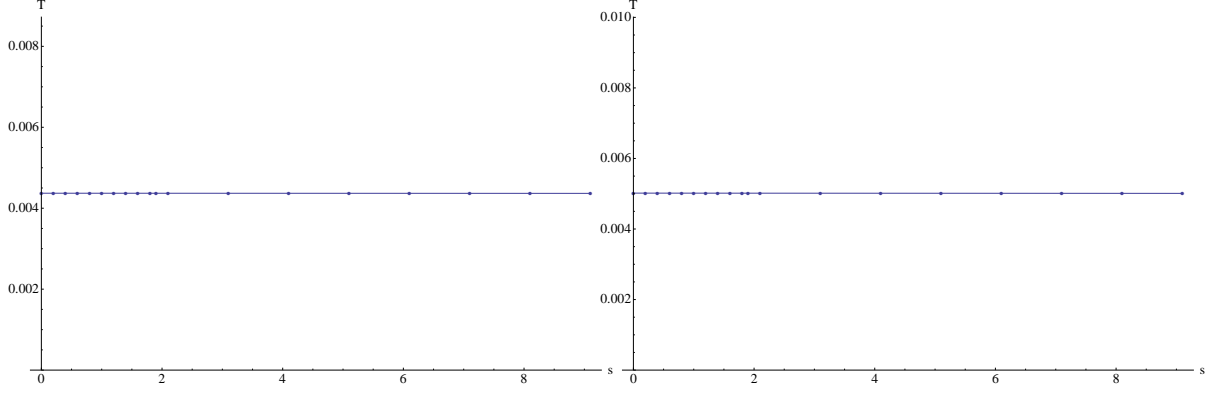


**Figure 5.** Temperature at the horizon versus  $N_f/N_c$ .  $c_+ = 50, C_2 = 5000$ . **Figure 6.** Temperature at the horizon versus  $N_f/N_c$ .  $c_+ = 3, C_2 = 800000$ .

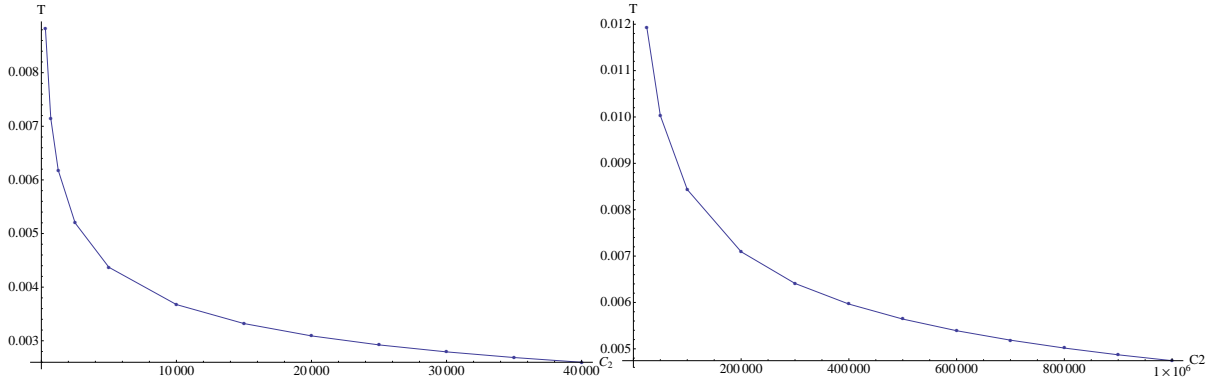


**Figure 7.** Temperature at the horizon versus  $C_2$ .  $c_+ = 50, s = 1$ . **Figure 8.** Temperature at the horizon versus  $C_2$ .  $c_+ = 3, s = 1$ .

## 4 Non-extremal backgrounds with flavored resolved deformed conifold asymptotics

In [15] the authors presented a solution generating technique that takes a IIB background of  $D5$  branes wrapped on the  $S^2$  of the resolved conifold (non-trivial  $F_3$  and  $\Phi$ ) and produces a background which also has  $D3$  charge (non trivial  $F_3, F_5, H_3$  and  $\Phi$ ). After a scaling limit the resulting geometry represents the baryonic branch of the Klebanov-Strassler solution. The initial space has topology  $R^{1,3} \times \mathcal{M}_6$  and preserves  $\mathcal{N} = 1$  supersymmetry. The algorithm consists of performing three T-dualities in the  $R^3$  directions, lifting to M-theory, boosting with rapidity  $\beta$  in the eleventh direction, reducing back to ten dimensions and finally T-dualizing back in  $R^3$ . This procedure is equivalent to a rotation in the space of Killing spinors. We will therefore refer to this

algorithm indistinctively as a *chain of dualities* or as a *rotation*.

In the previous section we found non-extremal solutions representing a background of  $N_c$  wrapped color  $D5$  branes and  $N_f$  smeared  $D5$  flavor branes ( $N_f/N_c \sim 1$ ). In this section we want to apply the procedure developed in [15] to these backgrounds.

After applying the rotation procedure, taking  $\beta \rightarrow \infty$  to decouple the gravitational modes, and performing the rescalings as described in [16], we obtain the transformed solutions in Einstein frame (see Appendix A for details):

$$\begin{aligned} ds_{IIB}^2 &= \tilde{N}\alpha' \left[ e^{-\phi/2} \mathcal{H}^{-1/2} (-e^{-8x} dt^2 + dx_i dx^i) + e^{3\phi/2} \mathcal{H}^{1/2} ds_6^2 \right], \\ F_3 &= \frac{\alpha' \tilde{N}}{4} f_3, \quad H_3 = -e^{-4x} \frac{\alpha' \tilde{N}}{4} e^{2\phi} *_6 f_3, \\ F_5 &= -(\alpha' \tilde{N})^2 (1 + *_{10}) \left[ \text{Vol}_{(4)} \wedge d \left( \frac{e^{-4x}}{\mathcal{H}} \right) \right], \end{aligned} \quad (4.1)$$

where

$$\mathcal{H}^{1/2} = \sqrt{e^{-2\phi} - e^{-8x}} \quad (4.2)$$

and  $ds_6^2$  is given in equation (2.14). Note that, unlike more standard finite temperature solutions where the non-extremality factor  $e^{-8x}$  enters only in the  $g_{rr}$  and  $g_{tt}$  elements of the metric, here the warp factor  $\mathcal{H}$  and the fluxes ( $F_5$  and  $H_3$ ) depend on  $e^{-8x}$ .<sup>6</sup>

The use of U-dualities is a well established solution generating technique in supergravity. In the presence of smeared flavored branes one could question the validity and meaning of the uplift to eleven dimensions. Two pieces of knowledge provide useful insight on this issue:

1. In [32] the authors studied the uplift of smeared  $D6$  flavor branes to M-theory. They argued that the violation of the Bianchi identity in ten dimensions implies that the eleven dimensional-geometry will no longer be Ricci flat; it is no longer of  $G_2$  holonomy but it does carry  $G_2$  structure. Thus, the flavors appear in eleven dimensions as intrinsic torsion. This eleven dimensional theory is no longer maximally supersymmetric (it is 1/8 BPS) and therefore it is no longer unique. This is an interesting possibility for the interpretation of the uplift of smeared flavor branes. For us, however, the important point is that once the reduction to ten dimensions is carried out the correct smearing form is recovered.

---

<sup>6</sup> Note also that in [16] the factor of  $e^{-8x}$  in  $H_3$  trivially cancelled with a similar one coming from the six dimensional Hodge dual. This is not the case here. The reason is that in [16] the authors considered a particular point in the baryonic branch ( $a = 0$ ) while in the present work we consider the general case,  $a(\rho)$  (see equation (A.4))



2. In [20] the authors studied a transformation to generate  $SU(3)$  structure solutions of IIB supergravity starting from non-Kähler backgrounds describing wrapped  $D5$  branes with additional flavor (smeared)  $D5$  branes. Working with the BPS equations and the  $SU(3)$  structure of the backgrounds they presented a solution generating technique that amounts to a rotation in the space of Killing spinors. This rotation procedure is well defined (even in the presence of smeared flavor branes) and is equivalent to the chain of U-dualities alluded to above.

In the present work we are dealing with a non-extremal deformation of [20]. However, since the backgrounds we are working with are not supersymmetric, we cannot use the BPS formalism of [20]. On the other hand, we are not interested in the interpretation of the background in eleven dimensions, so we will not attempt to address the questions presented in [32]. Instead, guided by the results of [20], we will forge ahead and apply the chain of dualities to the flavored, non extremal backgrounds with stabilized dilaton found in section 3. However in order to claim that the outcome of these dualities is still a solution of IIB plus sources, we have to show that the rotated backgrounds are indeed a solution of the EOMs.

#### 4.1 Equations of motion with $D3$ and $D5$ charges and smeared flavor branes

In this section we will verify that given the EOMs before the rotation procedure is applied, the EOMs after the rotation are also satisfied. The EOMs before rotation were presented in section 2.2 and derived in Appendix B. After the rotation procedure is carried out, the supergravity background contains  $H_3$  and  $F_5$  fluxes in addition to the  $F_3$  that was present before rotation. The full type IIB action, supplemented by the DBI action for the smeared flavor branes, is then given by

$$S = S_{IIB} + S_{\text{sources}} \quad (4.3)$$

where

$$S_{IIB} = \frac{1}{2\kappa_{10}^2} \int \sqrt{-g} R - \frac{1}{4\kappa_{10}^2} \int \left( d\phi \wedge *d\phi + e^{-\phi} H_{(3)} \wedge *H_{(3)} + e^{\phi} F_{(3)} \wedge *F_{(3)} + \frac{1}{2} F_{(5)} \wedge *F_{(5)} - C_{(4)} \wedge F_{(3)} \wedge H_{(3)} \right), \quad (4.4)$$

and

$$S_{\text{sources}} = -\frac{4T_5}{(4\pi)^2} \int \left( \text{Vol}_{(4)} \wedge d\rho \wedge d\psi e^{\phi/2} \sqrt{|g_{ab} + e^{-\phi/2} B_{ab}|} - C_{(6)} + C_{(4)} \wedge B_{(2)} \right) \wedge \Xi_{(4)} \quad (4.5)$$

Note that the metric is in Einstein frame and that  $g_{ab}$  and  $B_{ab}$  respectively represent the pullbacks of the metric and  $B_2$  to the flavor brane world volume. Recall that before rotation  $H_3 = 0$  and thus, the DBI action was only the pullback of the metric. After rotation we need to specify the form of the NS potential,  $B_2$ . In the extremal case ( $T = 0$ ), this potential should reduce to the one in [20]. We propose the following ansatz:

$$B_2 = b_1(\rho)\tilde{\omega}_3 \wedge d\rho + b_2(\rho)e_1 \wedge e_2 + b_3e_1 \wedge \tilde{\omega}_2 + b_4(\rho)e_2 \wedge \tilde{\omega}_1 + b_5(\rho)\tilde{\omega}_1 \wedge \tilde{\omega}_2. \quad (4.6)$$

To make the gauge degrees of freedom more apparent it is convenient to parameterize  $B_2$  in a slightly different way. Let us introduce  $b_2(\rho) = \tilde{b}_2(\rho) + (1 - a(\rho)^2)b_5(\rho)$ . It is then easy to verify that

$$B_2 = (B_2)_{b_5=0} - d[b_5(\rho)\tilde{\omega}_3] \quad (4.7)$$

with  $b_5(\rho)$  an undetermined function. It is clear that any  $b_5(\rho)$  results in the same  $H_3$ , and that  $b_5$  is just a gauge degree of freedom. Demanding that  $H_3 = d[B_2]$ , we get 5 equations. This system of equations can be reduced to just one differential equation. We choose a gauge such that  $b_1(\rho)$  coincides with the one in [20] (see Appendix D for details).

The flavor brane world volume is  $dt \wedge dx_1 \wedge dx_2 \wedge dx_3 \wedge d\rho \wedge d\psi \equiv \text{Vol}_{(4)} \wedge d\rho \wedge d\psi$ , and the smearing form is given by  $\Xi_{(4)} = \frac{s}{4} \sin \theta \sin \tilde{\theta} d\theta \wedge d\varphi \wedge d\tilde{\theta} \wedge d\tilde{\varphi}$ , where we have set  $\alpha' = g_s = 1$ . As was the case before rotation, the  $C_{(6)} \wedge \Xi_{(4)}$  term in the source action vanishes. Note that in the EOMs that follow from this action, the contribution from the Wess-Zumino term in the source action is exactly cancelled by that from the Chern-Simons term in the bulk.

The Bianchi identities for the RR and NS-NS forms after rotation are

$$dF_{(3)} = \Xi_{(4)}, \quad dH_{(3)} = 0, \quad dF_{(5)} + F_{(3)} \wedge H_{(3)} = B_{(2)} \wedge \Xi_{(4)} \quad (4.8)$$

The first is unchanged from before the rotation, and the latter two can be checked to hold given the EOMs before rotation. Note that this does not give us the full expression for  $B_{(2)}$ , but only the components which are orthogonal to  $\Xi_{(4)}$ , namely  $B_{\rho\psi}$ . However  $B_{(2)}$  only appears in the source action, and there it is either wedged with  $\Xi_{(4)}$ , or pulled back to the flavorbrane world volume (which is orthogonal to  $\Xi_{(4)}$ ). Therefore only this orthogonal component will be relevant for our equations of motion. A more detailed derivation of the general form of  $B_{(2)}$  is given in Appendix D.

The EOMs for the fluxes after rotation are

$$d(e^{-\phi} * H_{(3)}) = F_{(3)} \wedge F_{(5)} + \frac{e^{-8x}}{\mathcal{H}} \text{Vol}_{(4)} \wedge \Xi_{(4)} \quad (4.9)$$

$$d(e^\phi * F_{(3)}) = -H_{(3)} \wedge F_{(5)} \quad (4.10)$$

where the term with  $\mathcal{H}$  in the first equation comes from varying the source term. These can be checked to hold given the EOMs before rotation.

The dilaton EOM is

$$d(*d\phi) = \frac{e^\phi}{2} F_{(3)} \wedge *F_{(3)} - \frac{e^{-\phi}}{2} H_{(3)} \wedge *H_{(3)} + (2\kappa_{10}^2) \frac{\delta \mathcal{L}_{\text{sources}}}{\delta \phi}$$

where

$$\frac{\delta \mathcal{L}_{\text{sources}}}{\delta \phi} = \frac{1}{2} e^{\phi/2} \left( \sqrt{|g_{ab} + e^{-\phi/2} B_{ab}|} - \frac{|g_{(4)}| e^{-\phi} B_{\rho\psi}^2}{\sqrt{|g_{ab} + e^{-\phi/2} B_{ab}|}} \right) \text{Vol}_{(4)} \wedge d\rho \wedge d\psi \wedge \Xi_{(4)} \quad (4.11)$$

and can be checked to hold given the EOMs before rotation.

Lastly, we have the Einstein equations

$$\begin{aligned} R_{\mu\nu} - \frac{1}{2} g_{\mu\nu} R = & \frac{1}{2} \left( \partial_\mu \phi \partial_\nu \phi - \frac{1}{2} g_{\mu\nu} \partial_\lambda \phi \partial^\lambda \phi \right) + \frac{1}{12} e^\phi \left( 3F_{\mu\alpha\beta} F_\nu^{\alpha\beta} - \frac{1}{2} g_{\mu\nu} F_{(3)}^2 \right) \\ & + \frac{1}{12} e^{-\phi} \left( 3H_{\mu\alpha\beta} H_\nu^{\alpha\beta} - \frac{1}{2} g_{\mu\nu} H_{(3)}^2 \right) + \frac{1}{96} (F_{\mu\alpha\beta\gamma\delta} F_\nu^{\alpha\beta\gamma\delta}) + T_{\mu\nu}^{\text{sources}} \end{aligned} \quad (4.12)$$

where the variation of the Chern-Simons term in the bulk action is cancelled by the variation of the Wess-Zumino term in the source action. Here,  $T_{\mu\nu}^{\text{sources}}$  is obtained from (after rotation)

$$T_{\text{sources}}^{\mu\nu} = \frac{2\kappa_{(10)}^2}{\sqrt{-g_{(10)}}} \frac{\delta \mathcal{L}_{\text{sources}}}{\delta g_{\mu\nu}}, \quad (4.13)$$

and has components:

$$\begin{aligned} T_{tt}^{\text{sources}} &= \frac{s e^{-2g-2h-8x-4\phi}}{2\mathcal{H}^2}, & T_{x_i x_j}^{\text{sources}} &= -\frac{s \eta_{ij} e^{-2g-2h-4\phi}}{2\mathcal{H}^2}, \\ T_{\rho\rho}^{\text{sources}} &= -\frac{s}{2} e^{-2g-2h+2k+8x}, & T_{\psi\psi}^{\text{sources}} &= -\frac{s}{8} e^{-2g-2h+2k}, \\ T_{\varphi\psi}^{\text{sources}} &= -\frac{s}{8} e^{-2g-2h+2k} \cos \theta, & T_{\varphi\varphi}^{\text{sources}} &= -\frac{s}{8} e^{-2g-2h+2k} \cos^2 \theta, \\ T_{\tilde{\varphi}\psi}^{\text{sources}} &= -\frac{s}{8} e^{-2h-2g+2k} \cos \tilde{\theta}, & T_{\tilde{\varphi}\tilde{\varphi}}^{\text{sources}} &= -\frac{s}{8} e^{-2h-2g+2k} \cos^2 \tilde{\theta}, \\ T_{\varphi\tilde{\varphi}}^{\text{sources}} &= -\frac{s}{8} e^{-2h-2g+2k} \cos \theta \cos \tilde{\theta}. \end{aligned} \quad (4.14)$$

Again, the Einstein equations can be checked to hold given the EOMs before rotation.

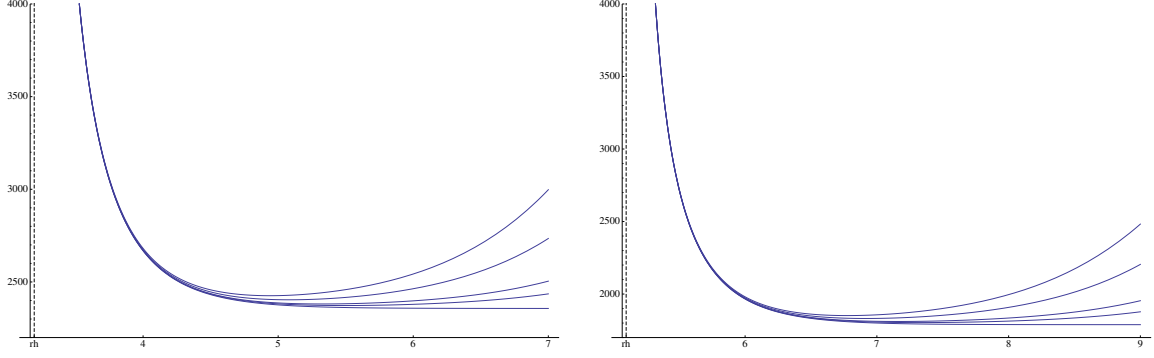


**Figure 9.**  $g_{\rho\rho}$  metric element for solutions after rotation,  $c_+ = 50$ ,  $C_2 = 5000$ . From bottom to top:  $s = 0, 1, 19/10, 51/10, 91/10$ . **Figure 10.**  $g_{\rho\rho}$  metric element for solutions after rotation,  $c_+ = 3$ ,  $C_2 = 800000$ . From bottom to top:  $s = 0, 1, 19/10, 51/10, 91/10$ .

## 4.2 Rotating flavored non-extremal solutions

It is now a simple procedure to use equations (4.1) along with our numerical solutions to produce the solutions after rotation. These are shown in Figs.(9 – 20)<sup>7</sup>; here the rotated metric has been written in the form

$$ds^2 = -g_{00}dt^2 + g_{xx}dx_id x^i + g_{\rho\rho}d\rho^2 + g_{\theta\theta}(e_1^2 + e_2^2) + g_{\tilde{\theta}\tilde{\theta}}(\tilde{\omega}_1^2 + \tilde{\omega}_2^2) + g_{\psi\psi}\tilde{\omega}_3^2. \quad (4.15)$$

In these plots, we show the  $c_+ = 3$  solutions out to a greater UV value than the  $c_+ = 50$  solutions because for large  $s$  values the dilaton does not stabilize as quickly for solutions with smaller  $c_+$

We note that the addition of flavor alters the behavior of the dilaton and the  $g_{xx}, g_{tt}, g_{\rho\rho}$  parts of the metric in the UV, but not in the IR. On the other hand, flavor affects the metric of the compact manifold at all energy scales, as shown in Figs.(15 – 20).

## 4.3 Asymptotics after the rotation

The rotation procedure changes the form of the UV asymptotics. The asymptotics of the rotated unflavored case were discussed in [16], but ours have a slightly different form due to differing signs for the  $C_2$  parameter. We define a quantity

$$c_+\sqrt{8}A(\rho) = \sqrt{24\rho + 8C_2c_+^2 - 3} \quad (4.16)$$

<sup>7</sup>The UV behavior of the rotated solutions is extremely sensitive to the precise UV behavior of the seed solutions, due to the  $\mathcal{H}$  factor. For this reason, we have generated these plots from the UV-shot seed solutions.

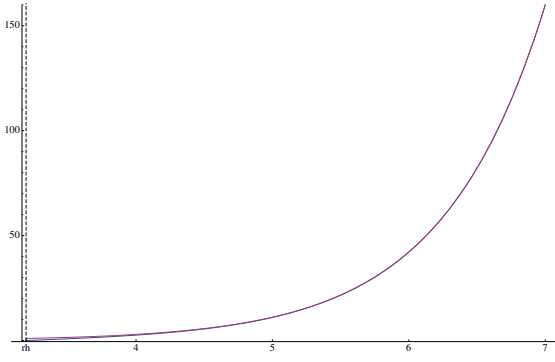


**Figure 11.**  $g_{xx}$  (red) and  $g_{tt}$  (blue) metric elements for the unflavored solution after rotation:  $c_+ = 50$ ,  $C_2 = 5000$ ,  $s = 0$ .

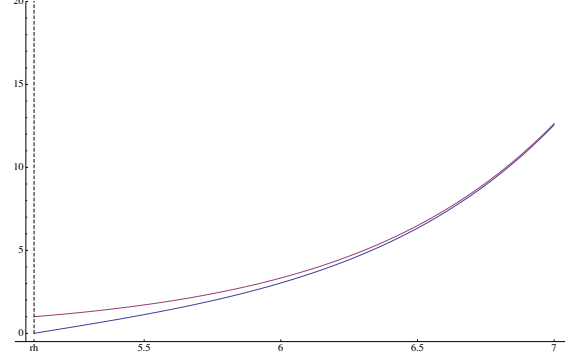


**Figure 12.**  $g_{xx}$  (red) and  $g_{tt}$  (blue) metric elements for the unflavored solution after rotation:  $c_+ = 3$ ,  $C_2 = 800000$ ,  $s = 0$ .

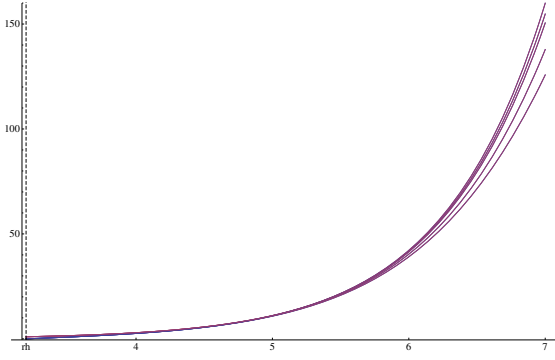


**Figure 13.**  $g_{xx}$  (red) and  $g_{tt}$  (blue) metric elements for flavored solutions after rotation:  $c_+ = 50$ ,  $C_2 = 5000$ . From top to bottom:  $c_+ = 3$ ,  $C_2 = 800000$ . From top to bottom:  $s = 0, 1, 19/10, 51/10, 91/10$ .

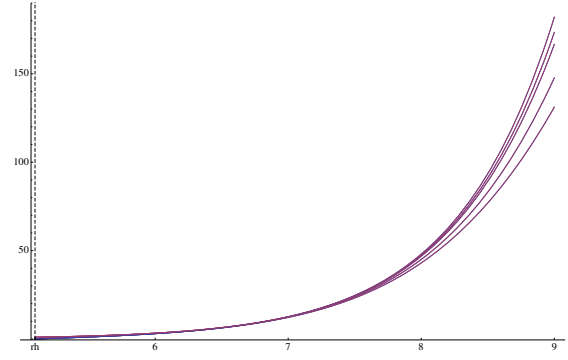


**Figure 14.**  $g_{xx}$  (red) and  $g_{tt}$  (blue) metric elements for flavored solutions after rotation:  $c_+ = 3$ ,  $C_2 = 800000$ . From top to bottom:  $s = 0, 1, 19/10, 51/10, 91/10$ .

in terms of which the unflavored UV asymptotics of the rotated metric functions become<sup>8</sup>

$$g_{xx} \sim \frac{e^{4\rho/3}}{A(\rho)} + \frac{e^{-4\rho/3}}{2048c^4A(\rho)^3} \left( 16c^2C_2(185 - 272\rho + 128\rho^2) + 3(-847 + 3504\rho - 3456\rho^2 + 2048\rho^3) \right) + \mathcal{O}(e^{-8\rho/3})$$

---

<sup>8</sup>Note that  $g_{tt} = -\tilde{\mathcal{H}}^{1/2}e^{-8x}$  after rotation.  $-g_{tt}$  below then gives the expansion of the positive expression  $\tilde{\mathcal{H}}^{1/2}e^{-8x}$ .

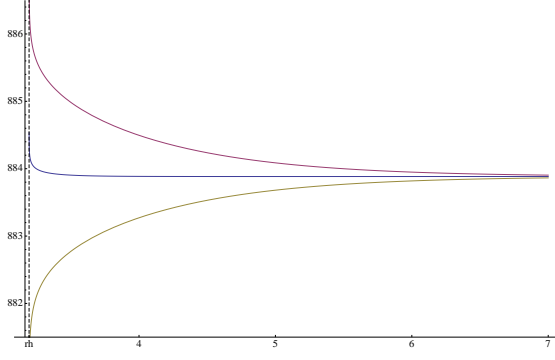


**Figure 15.**  $\frac{3}{2}g_{\psi\psi}$  (blue),  $g_{\theta\theta}$  (red), and  $g_{\tilde{\theta}\tilde{\theta}}$  (yellow) metric elements for unflavored solutions after rotation,  $c_+ = 50$ ,  $C_2 = 5000$ .

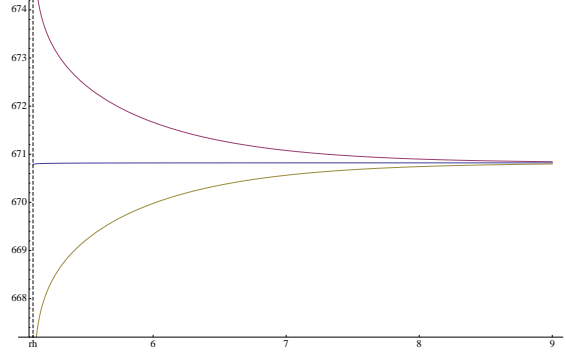


**Figure 16.**  $\frac{3}{2}g_{\psi\psi}$  (blue),  $g_{\theta\theta}$  (red), and  $g_{\tilde{\theta}\tilde{\theta}}$  (yellow) metric elements for unflavored solutions after rotation,  $c_+ = 3$ ,  $C_2 = 800000$ .

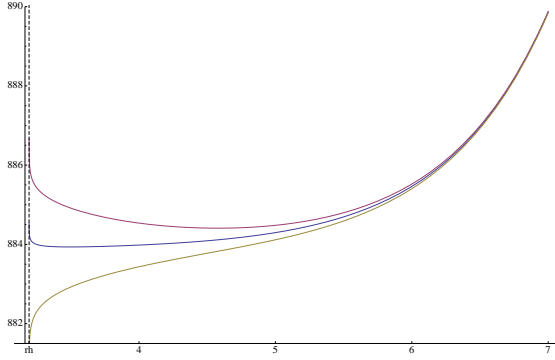


**Figure 17.**  $\frac{3}{2}g_{\psi\psi}$  (blue),  $g_{\theta\theta}$  (red), and  $g_{\tilde{\theta}\tilde{\theta}}$  (yellow) metric elements for flavored solution after rotation with  $s = 1/5$ ,  $c_+ = 50$ ,  $C_2 = 5000$ .

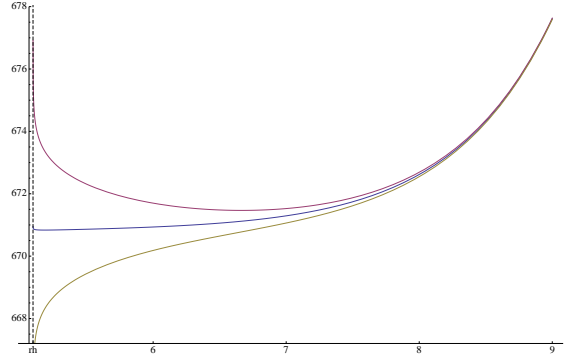


**Figure 18.**  $\frac{3}{2}g_{\psi\psi}$  (blue),  $g_{\theta\theta}$  (red), and  $g_{\tilde{\theta}\tilde{\theta}}$  (yellow) metric elements for flavored solution after rotation with  $s = 1/5$ ,  $c_+ = 3$ ,  $C_2 = 800000$ .

$$-g_{tt} \sim \frac{e^{4\rho/3}}{A(\rho)} + \frac{e^{-4\rho/3}}{2048c^4A(\rho)^3} \left( -2048c^4C_2^2 + 16c^2C_2(233 - 656\rho + 128\rho^2) + 3(-847 + 3504\rho - 3456\rho^2 + 2048\rho^3) \right) + \mathcal{O}(e^{-8\rho/3})$$

$$g_{\rho\rho} \sim \frac{2c}{3}A(\rho) + \mathcal{O}(e^{-8\rho/3}) \quad g_{\theta\theta} \sim \frac{c_+}{4}A(\rho) + \frac{e^{-4\rho/3}}{4}A(\rho)(2\rho - 1) + \mathcal{O}(e^{-8\rho/3})$$

$$g_{\psi\psi} \sim \frac{1}{6}cA(\rho) + \mathcal{O}(e^{-8\rho/3}) \quad g_{\tilde{\theta}\tilde{\theta}} \sim \frac{c_+}{4}A(\rho) - \frac{e^{-4\rho/3}}{4}A(\rho)(2\rho - 1) + \mathcal{O}(e^{-8\rho/3}).$$

(4.17)

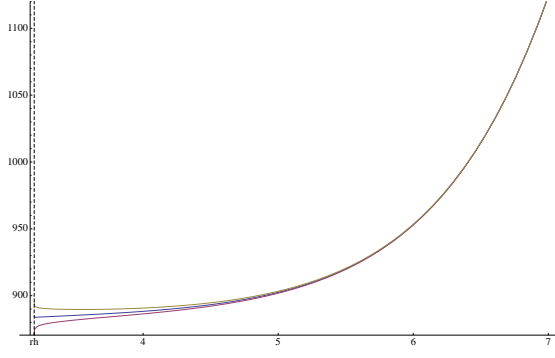


**Figure 19.**  $\frac{3}{2}g_{\psi\psi}$  (blue),  $g_{\theta\theta}$  (red), and  $g_{\tilde{\theta}\tilde{\theta}}$  (yellow) metric elements for flavored solution after rotation with  $s = 91/10$ ,  $c_+ = 50$ ,  $C_2 = 5000$ .

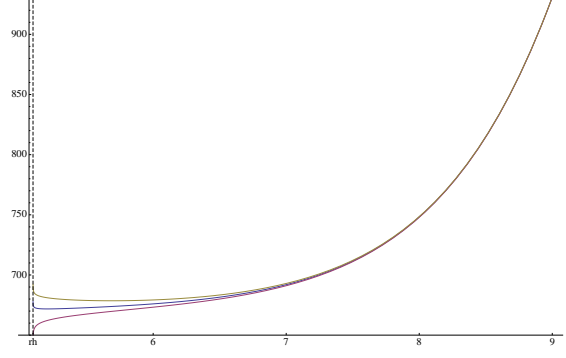


**Figure 20.**  $\frac{3}{2}g_{\psi\psi}$  (blue),  $g_{\theta\theta}$  (red), and  $g_{\tilde{\theta}\tilde{\theta}}$  (yellow) metric elements for flavored solution after rotation with  $s = 91/10$ ,  $c_+ = 3$ ,  $C_2 = 800000$ .

Using a variable  $u = e^{2\rho/3}$ , the metric reads at leading order

$$ds^2 = \frac{u^2}{A(u)}(dx_i dx^i) + \frac{3cA(u)}{2}\left(\frac{du^2}{u^2} + ds_{T^{11}}^2\right) + \dots \mathcal{O}(u^{-2}), \quad (4.18)$$

which is the asymptotic behavior of the Klebanov-Tseytlin background.

The addition of the smeared flavor branes causes the rotated asymptotics to depart drastically from the Klebanov-Tseytlin form in the UV. To first sub-leading order, we find

$$\begin{aligned} g_{xx} &\sim \frac{\sqrt{\frac{2c}{3}}e^{2\rho/3}}{\sqrt{s}} - \frac{e^{-2\rho/3}}{24\sqrt{6cs^{3/2}}} \left( 16c^2C_2 + 3(-2 + s(2 - 16\rho) + 16\rho + s^2(1 + 4\rho)) \right) + \dots \\ -g_{tt} &\sim \frac{\sqrt{\frac{2c}{3}}e^{2\rho/3}}{\sqrt{s}} - \frac{e^{-2\rho/3}}{24\sqrt{6cs^{3/2}}} \left( 16c^2C_2 + 3(-2 + s(2 - 16\rho) + 16\rho + s^2(1 + 4\rho)) \right) + \dots \\ g_{\rho\rho} &\sim \sqrt{\frac{2c}{3}}e^{2\rho/3}\sqrt{s} + \frac{e^{-2\rho/3}}{24\sqrt{6c}\sqrt{s}} \left( -6 + 16c^2C_2 + s(6 - 48\rho) + 48\rho + 3s^2(-11 + 4\rho) \right) + \dots \\ g_{\theta\theta} &\sim \sqrt{\frac{3c}{32}}e^{2\rho/3}\sqrt{s} + \frac{e^{-2\rho/3}}{64\sqrt{6c}\sqrt{s}} \left( -6 + 16c^2C_2 + s^2(9 - 36\rho) + 48\rho + 6s(-7 + 8\rho) \right) + \dots \\ g_{\tilde{\theta}\tilde{\theta}} &\sim \sqrt{\frac{3c}{32}}e^{2\rho/3}\sqrt{s} + \frac{e^{-2\rho/3}}{64\sqrt{6c}\sqrt{s}} \left( -6 + 16c^2C_2 + 48\rho - 18s(-3 + 8\rho) + s^2(-39 + 60\rho) \right) + \dots \\ g_{\psi\psi} &\sim \frac{\sqrt{ce^{2\rho/3}}\sqrt{s}}{2\sqrt{6}} + \frac{e^{-2\rho/3}}{96\sqrt{6c}\sqrt{s}} \left( -6 + 16c^2C_2 + s(6 - 48\rho) + 48\rho + 3s^2(-11 + 4\rho) \right) + \dots \end{aligned} \quad (4.19)$$

The leading order behavior of the metric functions for the compact and radial directions is now seen to be dominated by a term proportional to  $s^{1/2}$ . Looking at the metric for the Minkowski directions, we have leading order behavior proportional to  $s^{-1/2}$ , which shows that these asymptotic expansions diverge as  $s \rightarrow 0$  and in particular are not valid approximations for the UV behavior of solutions with  $s$  close but not equal to zero. Also, we clearly cannot regain the Klebanov-Tseytlin-like asymptotics of the unflavored solutions by taking  $s \rightarrow 0$  in these expressions — the exponential powers of  $\rho$  in the terms of the two series do not even agree. A different set of expressions, valid for  $s \sim 0$ , can be obtained by expanding around  $s = 0$  before performing the UV expansion of the rotated metric functions. These reduce to the unflavored asymptotics as  $s \rightarrow 0$ .

## 5 Energy and specific heat

In order to assess the thermodynamic stability of our solutions, we need to determine the specific heat,  $C_v$ . This is obtained from the expression for the ADM energy of our solutions and their temperature via the standard thermodynamic relation  $C_v = \partial E / \partial T$ .  $T$  is the numerically determined temperature given in equation (3.6), and  $E$  is given by the expression for the conserved ADM energy [33] (where  $16\pi G_{10} = 2\kappa_{10}^2 = (2\pi)^7$ )

$$E_{ADM} = -\frac{1}{8\pi G_{10}} \int_{S_t^\infty} \sqrt{|g_{00}|} ({}^8K - {}^8K_0) dS_t^\infty. \quad (5.1)$$

Here,  ${}^8K$  and  ${}^8K_0$  are the extrinsic curvatures of two 8-dimensional submanifolds  $S_t$  of  $\Sigma_t$  at constant  $\rho$ .  $\Sigma_t$  is a constant-time 9d spatial slice of the entire geometry, and we take for  $S_t$  the boundary manifold  $S_t^\infty$  as  $\rho \rightarrow \infty$ .  ${}^8K$  corresponds to our finite temperature backgrounds, whereas  ${}^8K_0$  is the extrinsic curvature of a reference background [33, 34]. For the reference background, we take one of the family of zero-temperature BPS solutions discussed in [20, 28]. The UV asymptotics of these backgrounds are summarized in Appendix C.2.

Our Euclideanized 10d metric reads

$$ds^2 = g_{00} d\tau^2 + g_{xx} dx_i dx^i + g_{\rho\rho} d\rho^2 + g_{\theta\theta} (e_1^2 + e_2^2) + g_{\tilde{\theta}\tilde{\theta}} (\tilde{\omega}_1^2 + \tilde{\omega}_2^2) + g_{\psi\psi} \tilde{\omega}_3^2. \quad (5.2)$$

The metric on a constant time slice  $\Sigma_t$ , and on its 8-dimensional boundary  $S_t^\infty$  are

$$ds_{\Sigma_t}^2 = g_{xx} dx_i dx^i + g_{\rho\rho} d\rho^2 + g_{\theta\theta} (e_1^2 + e_2^2) + g_{\tilde{\theta}\tilde{\theta}} (\tilde{\omega}_1^2 + \tilde{\omega}_2^2) + g_{\psi\psi} \tilde{\omega}_3^2 \quad (5.3)$$

$$ds_{S_t^\infty}^2 = g_{xx} dx_i dx^i + g_{\theta\theta} (e_1^2 + e_2^2) + g_{\tilde{\theta}\tilde{\theta}} (\tilde{\omega}_1^2 + \tilde{\omega}_2^2) + g_{\psi\psi} \tilde{\omega}_3^2, \quad (5.4)$$



where the metric functions in Einstein frame are

$$\begin{aligned}
g_{00} &= e^{\phi/2} e^{-8x} & g_{00_B} &= e^{\phi_B/2} \nu_B \\
g_{xx} &= e^{\phi/2} & g_{xx_B} &= e^{\phi_B/2} \\
g_{\rho\rho} &= e^{\phi/2} e^{8x} e^{2k} & g_{\rho\rho_B} &= e^{\phi_B/2} e^{2k_B} \\
g_{\theta\theta} &= e^{\phi/2} e^{2h} & g_{\theta\theta_B} &= e^{\phi_B/2} e^{2h_B} \\
g_{\tilde{\theta}\tilde{\theta}} &= \frac{1}{4} e^{\phi/2} e^{2g} & g_{\tilde{\theta}\tilde{\theta}_B} &= \frac{1}{4} e^{\phi_B/2} e^{2g_B} \\
g_{\psi\psi} &= \frac{1}{4} e^{\phi/2} e^{2k} & g_{\psi\psi_B} &= \frac{1}{4} e^{\phi_B/2} e^{2k_B}
\end{aligned} \tag{5.5}$$

before rotation, and

$$\begin{aligned}
g_{00} &= e^{-\phi/2} \mathcal{H}^{-1/2} e^{-8x} & g_{00_B} &= e^{-\phi_B/2} \mathcal{H}_B^{-1/2} \nu_B \\
g_{xx} &= e^{-\phi/2} \mathcal{H}^{-1/2} & g_{xx_B} &= e^{-\phi_B/2} \mathcal{H}_B^{-1/2} \\
g_{\rho\rho} &= e^{3\phi/2} \mathcal{H}^{1/2} e^{8x} e^{2k} & g_{\rho\rho_B} &= e^{3\phi_B/2} \mathcal{H}_B^{1/2} e^{2k_B} \\
g_{\theta\theta} &= e^{3\phi/2} \mathcal{H}^{1/2} e^{2h} & g_{\theta\theta_B} &= e^{3\phi_B/2} \mathcal{H}_B^{1/2} e^{2h_B} \\
g_{\tilde{\theta}\tilde{\theta}} &= \frac{1}{4} e^{3\phi/2} \mathcal{H}^{1/2} e^{2g} & g_{\tilde{\theta}\tilde{\theta}_B} &= \frac{1}{4} e^{3\phi_B/2} \mathcal{H}_B^{1/2} e^{2g_B} \\
g_{\psi\psi} &= \frac{1}{4} e^{3\phi/2} \mathcal{H}^{1/2} e^{2k} & g_{\psi\psi_B} &= \frac{1}{4} e^{3\phi_B/2} \mathcal{H}_B^{1/2} e^{2k_B}
\end{aligned} \tag{5.6}$$

after rotation; ‘ $B$ ’ subscripts indicate the BPS backgrounds. Here  $\mathcal{H} = (e^{-2\phi} - e^{-8x})$  and  $\mathcal{H}_B = (e^{-2\phi_B} - \kappa_2^2)$ , where  $\kappa_2$  is a free parameter with  $0 < \kappa_2 < e^{-\phi_\infty}$  that parametrizes the rotation, see [20]. In terms of the 11d boost parameter  $\beta$ , we have  $\kappa_2 = e^{-\phi_\infty} \tanh \beta$ . Note that for the BPS solutions  $e^{-8x} = 1$ , and we have also allowed for an arbitrary rescaling of the  $\tau$  coordinate via a constant parameter  $\nu_B$ , reflecting the freedom in choosing the period  $\beta$  of the Euclidean time coordinate for these backgrounds.

It is now straightforward to calculate the extrinsic curvature of an 8-manifold  $S_t$  at constant  $\rho$ . We obtain

$${}^8K_{bef} = e^{-\frac{\phi(\rho)}{4} - k(\rho) - 4x(\rho)} (2\phi'(\rho) + 2g'(\rho) + 2h'(\rho) + k'(\rho)) \tag{5.7}$$

for the background before rotation, and

$$\begin{aligned}
{}^8K_{aft} &= \frac{1}{2} \frac{\mathcal{H}(\rho)}{\mathcal{H}(\rho)^{5/4}} e^{-\frac{3\phi(\rho)}{4} - k(\rho) - 4x(\rho)} \\
&+ \frac{1}{\mathcal{H}(\rho)^{1/4}} e^{-\frac{3\phi(\rho)}{4} - k(\rho) - 4x(\rho)} \left( 3\phi'(\rho) + 2g'(\rho) + 2h'(\rho) + k'(\rho) \right)
\end{aligned} \tag{5.8}$$

for the rotated background.<sup>9</sup>

The expressions for  $dS_t$  are

$$dS_{t_{bef}} = \frac{1}{8} e^{2\phi} e^{2g+2h+k} dV_3 \wedge dS_{\mathcal{M}_6} \quad dS_{t_{aft}} = \frac{1}{8} \mathcal{H}^{1/2} e^{3\phi} e^{2g+2h+k} dV_3 \wedge dS_{\mathcal{M}_6} \quad (5.9)$$

where  $dV_3 = dx_1 \wedge dx_2 \wedge dx_3$  is the volume form on the Minkowski spatial directions, and  $dS_{\mathcal{M}_6} = (\sin \theta \sin \tilde{\theta}) d\theta \wedge d\varphi \wedge d\tilde{\theta} \wedge d\tilde{\varphi} \wedge d\psi$  is the volume form on the compact cycles. Putting all of these together and integrating over the compact  $\theta, \varphi, \tilde{\theta}, \tilde{\varphi}, \psi$  directions we obtain expressions for the ADM energy before and after the rotation:

$$e_{bef} = \frac{E_{bef}}{V_3} = -\frac{1}{8\pi^4} \left[ e^{-8x} e^{2\phi+2g+2h} \left( 2(\phi' + g' + h') + k' \right) - \sqrt{\nu_B} e^{2\phi_B+2g_B+2h_B} \left( 2(\phi'_B + g'_B + h'_B) + k'_B \right) \right] \Big|_{\rho \rightarrow \infty} \quad (5.10)$$

$$e_{aft} = -\frac{1}{8\pi^4} \left[ e^{-8x} e^{2\phi+2g+2h} \left( \frac{\mathcal{H}'}{2\mathcal{H}} + (3\phi' + 2(g' + h') + k') \right) - \sqrt{\nu_B} e^{2\phi_B+2g_B+2h_B} \left( \frac{\mathcal{H}'_B}{2\mathcal{H}_B} + (3\phi'_B + 2(g'_B + h'_B) + k'_B) \right) \right] \Big|_{\rho \rightarrow \infty} \quad (5.11)$$

Here  $V_3 = \text{Vol}(R^3)$ , and we have expressed the results as energy densities per unit flat 3-volume.

We evaluate these expressions at a large but finite value of  $\rho = \rho_*$  by inserting the UV asymptotics of the BPS and finite temperature solutions. The BPS asymptotics are given in terms of the free variables  $Q_o, c_+, c_-, \rho_0$  and  $f_{1,0}$ , and are listed in Appendix C.2. The finite temperature asymptotics were given in section 3.1, and are a deformation of a BPS background with  $Q_o = -N_c + N_f/2$  and  $\rho_0 = 0$ .

In order to calculate the ADM energy, we first match the geometries and matter fields of the BPS and finite temperature backgrounds at  $\rho_*$ , this amounts to matching the metric functions  $g_{00}, g_{xx}, g_{\theta\theta}, g_{\tilde{\theta}\tilde{\theta}}, g_{\psi\psi}$ , as well as the dilaton. Only after this matching is performed we let  $\rho_* \rightarrow \infty$ .

We begin with the case before rotation. To avoid confusion with the parameters  $c_+$  and  $c_-$  in the finite temperature solutions, we will write the BPS  $c_+$  and  $c_-$  parameters in bold as  $\mathbf{c}_+$  and  $\mathbf{c}_-$ . First we pick some fixed values of  $c_+, C_2$  and  $s$  to specify the finite temperature background. We begin the matching by using the freedom in  $\nu_B$  to set  $\nu_B = e^{-8x(\rho_*)}$ . Next we match  $e^{\phi/2} = e^{\phi_B/2}$  to  $\mathcal{O}(e^{-12\rho_*/3})$  by setting

$$f_{1,0} = 1 - e^{-12\rho_*/3} \frac{C_2 s}{c_+}. \quad (5.12)$$

---

<sup>9</sup>The BPS backgrounds will have  $e^{-4x} = 1$ .

As a result,  $g_{00}$  and  $g_{xx}$  are now matched to  $\mathcal{O}(e^{-12\rho_*/3})$ . Now, we match  $e^{2k} = e^{2k_B}$ ,  $e^{2h} = e^{2h_B}$ , and  $e^{2g} = e^{2g_B}$ , respectively, to  $\mathcal{O}(e^{-8\rho_*/3})$ , by setting

$$\begin{aligned} \mathbf{c}_+ &= c_+ + e^{-12\rho_*/3} \frac{11C_2s}{48} \\ Q_0 &= -1 + \frac{s}{2} - \frac{1}{16} e^{-8\rho_*/3} C_2(-5 + 4\rho_*)(-2 + s) \\ \mathbf{c}_- &= \frac{2}{3} c_+^2 (-11C_2s + 4C_2s\rho_*), \end{aligned} \tag{5.13}$$

which results in the matching of  $g_{\theta\theta}$ ,  $g_{\tilde{\theta}\tilde{\theta}}$ ,  $g_{\psi\psi}$  to  $\mathcal{O}(e^{-8\rho_*/3})$ .

With these definitions, the dilaton and all of the metric functions  $g_{00}$ ,  $g_{xx}$ ,  $g_{\theta\theta}$ ,  $g_{\tilde{\theta}\tilde{\theta}}$ ,  $g_{\psi\psi}$  are matched up to (at least)  $\mathcal{O}(e^{-8\rho_*/3})$ . The freedom in the  $\rho_0$  parameter in the BPS solutions is not needed, and we set it equal to zero as was done for the finite temperature solutions. Taking  $\rho_* \rightarrow \infty$ , the resulting ADM energy density is finite, independent of  $s$ , and equal to

$$e_{bef} = \frac{5c_+^2 C_2}{96\pi^4} \tag{5.14}$$

After the rotation, the presence of  $\mathcal{H}$  causes the mixing of the UV asymptotics in the metric functions to become slightly more involved. The rotation also causes the metric function expansions to become unwieldy at higher order, so we only perform the matching to  $\mathcal{O}(e^{-2\rho_*})$  which is enough to render the ADM energy finite. Despite these technical complications the process proceeds as above. Namely, before taking the  $\rho_* \rightarrow \infty$  limit we fix coefficients so that the BPS and finite temperature metrics match at the boundary, we then take the  $\rho_* \rightarrow \infty$  limit and obtain a finite energy given by

$$e_{aft} = \frac{5c_+^2 C_2}{96\pi^4}. \tag{5.15}$$

Thus, the energy remains the same as before the rotation.

The above analysis was done for flavored finite-temperature backgrounds with  $s \neq 0$ . However, since the results do not depend on  $s$  they should also hold for backgrounds without flavor *i.e* for non-extremal deformations that, after the rotation, do have Klebanov-Strassler asymptotics. We have explicitly checked that this is indeed the case.

In Fig. (21) we plot  $de/d\mathfrak{s}$ <sup>10</sup> and  $T$  as functions of the entropy density (or equivalently the “radius” of the horizon) for solutions before the rotation. The overlap of the two curves show that the numerical solutions satisfy the first law of thermodynamics

$$de = Td\mathfrak{s}. \tag{5.16}$$

---

<sup>10</sup>  $\mathfrak{s}$  denotes the entropy density  $S/V_3$  and should not be confused with the flavor parameter  $s$ .

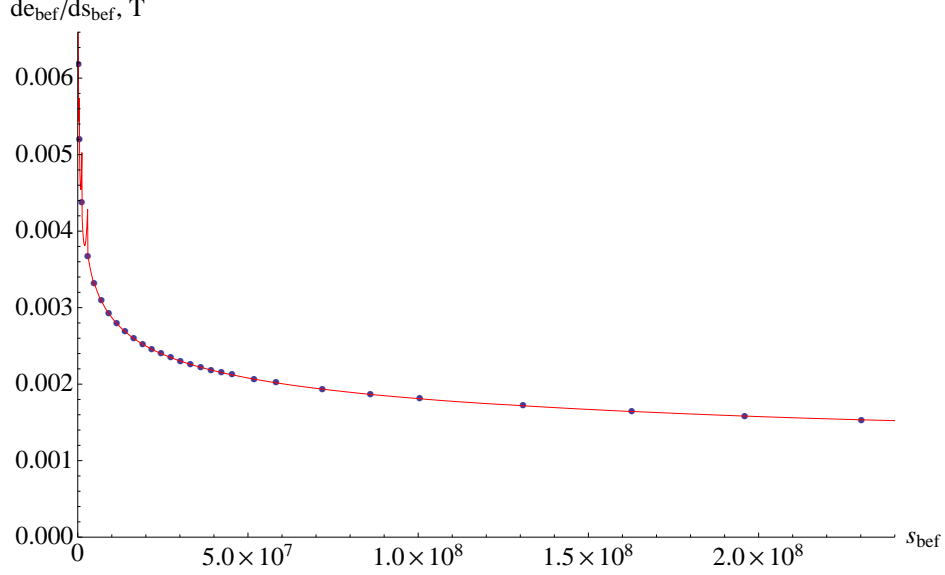


**Figure 21.**  $de_{bef}/ds_{bef}$  (red line) and  $T_h$  (blue dots) plotted vs.  $s_{bef}$ , for the flavored case with  $c_+ = 50$ ,  $s = 1$ .

To verify that this is also the case after the rotation recall that we have already shown that the temperature and energy density remain the same (5.14),(5.15),(3.6). It is easy to see that the entropy density is also unaffected by the rotation,

$$s_{bef} = \frac{S_{bef}}{V_3} = \frac{e^{2\phi} e^{2h+2g+k}}{4\pi^3} \Big|_{\rho=\rho_h} \quad (5.17)$$

$$s_{aft} = \frac{S_{aft}}{V_3} = \frac{e^{3\phi} \mathcal{H}^{1/2} e^{2h+2g+k}}{4\pi^3} \Big|_{\rho=\rho_h} = \frac{e^{3\phi} (e^{-2\phi} - e^{-8x})^{1/2} e^{2h+2g+k}}{4\pi^3} \Big|_{\rho=\rho_h} = s_{bef} \quad (5.18)$$

where the last equality in equation (5.18) follows from the fact that  $e^{-8x}$  vanishes at the horizon.

Thus, the thermodynamical quantities  $e$ ,  $s$  and  $T$  are not modified by the rotation and the first law will still hold.

As discussed in section 3.4, our numerics associate a horizon temperature with a choice of  $c_+$  and  $C_2$ . In Figs.(22) and (23) we plot the energy density versus the associated temperature for a solution with  $s = 1$ . The slope of these plots is the specific heat  $C_v$  and is seen to be negative both before and after the rotation. Note that the fact that the first law is satisfied implies that we would have gotten the same answer had we chosen to use holographic renormalization methods.

The backreaction of the flavor branes does not play any role in the stability analysis as the temperature's dependence on  $s$  is essentially negligible compared to its dependence on  $C_2$  and neither the energy nor the entropy depend on  $s$ . In Figs.(24) and (25) we show the energy density versus the entropy density  $S/V_3$ . Note that in Figs.(24) and (25) the behavior of the energy vs. entropy is linear for large values of  $S$  (or equivalently for large values of the horizon “radius”). From the first law of thermodynamics,  $dE = TdS$ , we expect this to happen when the temperature is constant.

Thus, we have shown that, despite of having very different asymptotics, the backgrounds after the rotation have thermodynamical properties similar to the  $D5$  wrapped branes system.

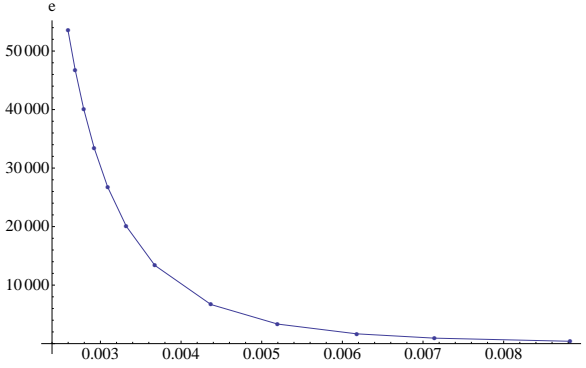


**Figure 22.** ADM energy density versus horizon temperature ( $s = 1$ ,  $c_+ = 50$ )

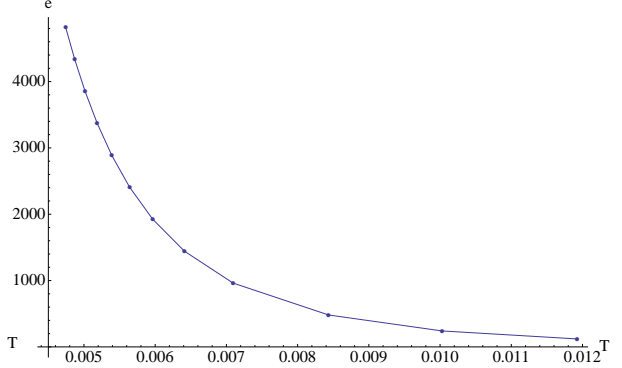


**Figure 23.** ADM energy density versus horizon temperature ( $s = 1$ ,  $c_+ = 3$ )

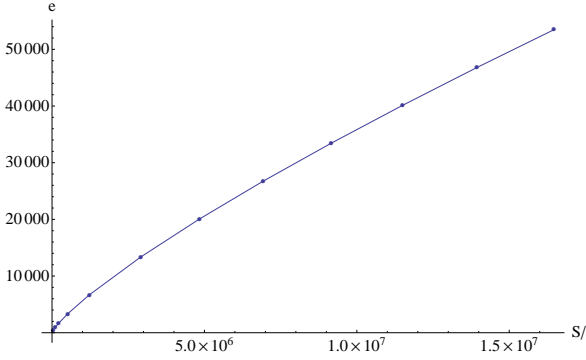


**Figure 24.** ADM energy density versus entropy density ( $s = 1$ ,  $c_+ = 50$ )

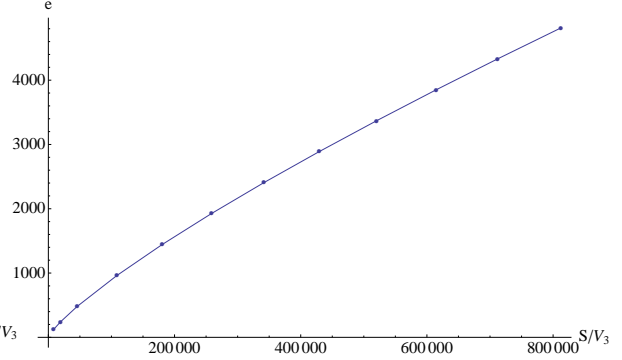


**Figure 25.** ADM energy density versus entropy density ( $s = 1$ ,  $c_+ = 3$ )

## 6 Conclusions

Let us summarize the main points of this paper.

- We found finite temperature solutions describing  $N_c$  D5 branes wrapped on the  $S^2$  of the resolved conifold. Unlike the generic wrapped D5 branes backgrounds the ones presented here have a dilaton that does not blow up at infinity but stabilizes to a finite value.
- We identify a set of 11 UV and 6 IR parameters that determine the asymptotics of the solutions to *any* order.
- It was not our goal to explore all the possible families of solutions in the 17 parameter space but to restrict ourselves to those that have a UV behavior similar to the ones in [20]. Therefore, we fixed several of the UV parameters to appropriate values. We then solved the EOM's numerically using these UV expansions as boundary conditions and demanding regularity at the horizon. We also imposed that the constraint coming from reparametrization invariance is satisfied, to order  $10^{-6}$  or better, throughout all the interval.
- Using U-dualities and these backgrounds as “seeds” we generate solutions with  $D3$  and  $D5$  charge. To avoid issues related to the uplift of the smeared flavor branes, we show explicitly that after the U-dualities are applied the background obtained is a solution of the EOM's of  $D3$  and  $D5$  brane sources.
- In the absence of temperature the backgrounds obtained are dual to interesting field theories that exhibit Seiberg dualities, Higgsing and confinement [20]. It is tempting to think of the non-extremal solutions found here as dual to finite temperature versions of the field theories in [20]. However, for non-zero temperature we have to first study the thermodynamical stability. We proceed to do that and find that the specific heat is negative and thus, they are unstable.
- The backgrounds studied here are more general and in several ways different than the finite temperature Maldacena-Nuñez considered in [35]. In particular, after the rotation they have a very different (Klebanov-Strassler-like) asymptotics. However, the negative specific heat seems to indicate that the tachyonic mode found in [35] is still present.
- The solutions in [16] are a particular case (no flavor,  $a(\rho)=0$ ) of ours, thus the thermodynamical instability found here applies also to [16]. This indicates that the hope of achieving stable Klebanov-Strassler black holes starting with wrapped

$D5$  and using U-dualities is not realized; the solutions seem to inherit the instability of the wrapped  $D5$  solutions.

In [20],[21],[22],[23] it was shown that solutions of type IIB supergravity with sources generalize the Klebanov-Strassler baryonic branch; the dual field theory exhibits Seiberg dualities, Higgsing and confinement at different scales. One of the motivations of the present work was to find gravity duals of these interesting field theories. We find that starting from non-extremal wrapped  $D5$  branes and applying the same dualities used to generate the extremal backgrounds produces thermodynamically unstable backgrounds. What is then the finite temperature gravity dual of the field theories found in [20],[21],[22],[23]? This fascinating question will undoubtedly lead to interesting physics and remains open.

## 7 Acknowledgments

We thank Carlos Nuñez for many useful discussions, correspondence and comments. We also thank Alex Buchel and Leopoldo Pando Zayas for comments on this manuscript. The work of E.C. and S.Y. is partially supported by the National Science Foundation under Grant No. PHY-0969020. E.C. also acknowledges support of CONACyT grant CB-2008-01-104649 and CONACyT's High Energy Physics Network.

## A Appendix: U-Duality for the flavored, wrapped $D5$ branes black hole

Here we describe in more detail the steps of the U-duality procedure as applied to backgrounds of the type mentioned in equations (2.14) and (2.13). We will consider the rotation in string frame. We begin with

$$\begin{aligned}
ds_{IIB}^2 &= e^{\phi(\rho)} \left[ -e^{-8x(\rho)} dt^2 + dx_1^2 + dx_2^2 + dx_3^2 \right] + ds_6^2, \\
ds_6^2 &= e^{\phi(\rho)} \left[ e^{8x(\rho)} e^{2k(\rho)} d\rho^2 + e^{2h(\rho)} (d\theta^2 + \sin^2 \theta d\varphi^2) \right. \\
&\quad + \frac{e^{2g(\rho)}}{4} \left( (\omega_1 + a(\rho) d\theta)^2 + (\omega_2 - a(\rho) \sin \theta d\varphi)^2 \right) \\
&\quad \left. + \frac{e^{2k(\rho)}}{4} (\omega_3 + \cos \theta d\varphi)^2 \right], \tag{A.1}
\end{aligned}$$

and

$$F_{(3)} = \frac{N_c}{4} \left[ -(\omega_1 + b(\rho)d\theta) \wedge (\omega_2 - b(\rho)\sin\theta d\varphi) \wedge (\omega_3 + \cos\theta d\varphi) + \right. \\ \left. b'd\rho \wedge (-d\theta \wedge \omega_1 + \sin\theta d\varphi \wedge \omega_2) + (1 - b(\rho)^2 - \frac{N_f}{N_c}) \sin\theta d\theta \wedge d\varphi \wedge \omega_3 \right]. \quad (\text{A.2})$$

We will write  $\phi = f$  to avoid confusion with the transformed dilaton and will suppress obvious  $\rho$  dependence to avoid cluttering. We begin by T-dualizing in the  $x_1, x_2, x_3$  directions, which results in the type IIA background

$$ds_{IIA}^2 = e^f \left[ -e^{-8x} dt^2 \right] + e^{-f} (dx_1^2 + dx_2^2 + dx_3^2) + ds_6^2, \\ e^{2\phi_A} = e^{2\phi - 3f}, \\ F_6 = F_3 \wedge dx_1 \wedge dx_2 \wedge dx_3 \rightarrow F_4 = e^{2f} e^{-4x} *_6 F_3 \wedge dt. \quad (\text{A.3})$$

where

$$*_6 F_3 = \frac{N_c e^{4x}}{8} \left\{ - \left[ e^{2g-2h} a^2 (1 + a^2 - 2ab - s) + 16e^{2h-2g} + 8a(a-b) \right] e_1 \wedge e_2 \wedge d\rho \right. \\ + \left[ e^{2g-2h} a (1 + a^2 - 2ab - s) + 4(a-b) \right] (e_1 \wedge \omega_2 + e_2 \wedge \omega_1) \wedge d\rho \\ + e^{2g-2h} (1 + a^2 - 2ab - s) (\omega_1 \wedge \omega_2 \wedge d\rho) \\ \left. + e^{-8x} b' (e_1 \wedge \omega_1 + e_2 \wedge \omega_2) \wedge \tilde{\omega}_3 \right\}. \quad (\text{A.4})$$

Now, we lift this to M-theory:

$$ds_{11}^2 = e^{4\phi/3-2f} dx_{11}^2 + e^{f-2\phi/3} \left[ -e^{-8x} e^f dt^2 + e^{-f} (dx_1^2 + dx_2^2 + dx_3^2) + ds_6^2 \right], \\ G_4 = e^{-4x} e^{2f} *_6 F_3 \wedge dt. \quad (\text{A.5})$$

Boosting in the  $(t, x_{11})$  directions according to

$$dt \rightarrow \cosh \beta dt - \sinh \beta dx_{11}, \quad dx_{11} \rightarrow -\sinh \beta dt + \cosh \beta dx_{11}, \quad (\text{A.6})$$

we rewrite the boosted metric as

$$ds_{11}^2 = e^{f-2\phi/3} \left[ e^{-f} (dx_1^2 + dx_2^2 + dx_3^2) + ds_6^2 \right] + A dt^2 + B dx_{11}^2 + C dt dx_{11}, \\ G_4 = e^{-4x} e^{2f} *_6 F_3 \left[ \cosh \beta dt - \sinh \beta dx_{11} \right] \quad (\text{A.7})$$



where

$$\begin{aligned} A &= e^{2f-2\phi/3}[\sinh^2 \beta e^{2\phi-4f} - e^{-8x} \cosh^2 \beta], \quad B = e^{2f-2\phi/3}[\cosh^2 \beta e^{2\phi-4f} - e^{-8x} \sinh^2 \beta], \\ C &= -2 \cosh \beta \sinh \beta e^{2f-2\phi/3}[e^{2\phi-4f} - e^{-8x}]. \end{aligned} \quad (\text{A.8})$$

Before reducing to IIA, it is useful to write equation (A.7) as

$$\begin{aligned} ds_{11}^2 &= B^{-1/2} \left[ g_{tt} dt^2 + B^{1/2} e^{f-2\phi/3} (e^{-f} (dx_1^2 + dx_2^2 + dx_3^2) + ds_6^2) \right] + B(dx_{11} + a_t dt)^2, \\ G_4 &= e^{-4x} e^{2f} *_6 F_3 \left[ (\cosh \beta + a_t \sinh \beta) dt - \sinh \beta (dx_{11} + a_t dt) \right] \end{aligned} \quad (\text{A.9})$$

where we have defined

$$a_t = \frac{C}{2B}, \quad g_{tt} = \frac{4AB - C^2}{4\sqrt{B}}, \quad e^{4\phi_A/3} = B. \quad (\text{A.10})$$

Now we reduce to IIA, obtaining in string frame,

$$\begin{aligned} ds_{IIA}^2 &= g_{tt} dt^2 + \sqrt{B} e^{-2\phi/3} (dx_1^2 + dx_2^2 + dx_3^2) + \sqrt{B} e^{f-2\phi/3} ds_6^2, \\ e^{2\phi_A} &= B^{3/2}, \\ F_4 &= e^{-4x} e^{2f} *_6 F_3 \wedge \left[ (\cosh \beta + a_t \sinh \beta) dt \right], \\ H_3 &= -\sinh \beta e^{-4x} e^{2f} *_6 F_3, \\ F_2 &= a'_t d\rho \wedge dt. \end{aligned} \quad (\text{A.11})$$

Next, we T-dualize back along the  $x_1, x_2, x_3$  directions, and obtain

$$\begin{aligned} ds_{IIB}^2 &= g_{tt} dt^2 + \frac{e^{2\phi/3}}{\sqrt{B}} (dx_3^2 + dx_1^2 + dx_2^2) + \sqrt{B} e^{f-2\phi/3} ds_6^2, \\ e^{2\phi_B} &= e^{2\phi}, \\ F_7 &= e^{-4x} e^{2f} *_6 F_3 \wedge \left[ (\cosh \beta + a_t \sinh \beta) dt \right] \wedge dx_3 \wedge dx_2 \wedge dx_1 \quad F_3 = *_{10} F_7, \\ H_3 &= -\sinh \beta e^{-4x} e^{2f} *_6 F_3, \\ F_5 &= a'_t d\rho \wedge dt \wedge dx_3 \wedge dx_2 \wedge dx_1 (1 + *_{10}). \end{aligned} \quad (\text{A.12})$$

Finally we set  $f = \phi$ , use the definitions for  $A, B, C$  and  $a_t$ , and take the limit  $\beta \rightarrow \infty$ . This is the field theory limit, where the warp factors vanish at infinity. We then rescale

$$\tilde{N} = N \cosh \beta, \quad x_i \rightarrow \sqrt{\cosh \beta} \sqrt{\tilde{N} \alpha'} x_i. \quad (\text{A.13})$$

With all of the above, the  $\beta \rightarrow \infty$  limits are finite and the final solution is given by equations (4.1) and (4.2) after transforming to Einstein frame.

## B Appendix: The equations of motion

In this appendix we briefly review the metric ansatz and solution method of [31], which we use to derive the Einstein equations and constraint given in section 2.2 for the flavored non-extremal backgrounds before rotation.

The metric ansatz in [31], in Einstein frame, reads

$$ds_{IIB}^2 = -Y_1 dt^2 + Y_2(dx_1^2 + dx_2^2 + dx_3^2) + Y_3 d\rho^2 + Y_4(d\theta^2 + \sin^2 \theta d\varphi^2) \\ + Y_5(\omega_1 + a d\theta)^2 + (\omega_2 - a \sin \theta d\varphi)^2 + Y_6(\omega_3 + \cos \theta d\varphi)^2.$$

The  $F_3$  gauge field ansatz is given by

$$F_{(3)} = \frac{N_c}{4} \left[ -(\omega_1 + b d\theta) \wedge (\omega_2 - b \sin \theta d\varphi) \wedge (\omega_3 + \cos \theta d\varphi) \right. \\ \left. + b' dr \wedge (-d\theta \wedge \omega_1 + \sin \theta d\varphi \wedge \omega_2) + \left( 1 - b^2 - \frac{N_f}{N_c} \right) \sin \theta d\theta \wedge d\varphi \wedge \omega_3 \right]. \quad (\text{B.1})$$

where the  $Y_i$ ,  $a$ , and  $b$  are functions of  $\rho$  only.

The complete action for type IIB supergravity with smeared flavor branes is then

$$S = S_{\text{grav}} + S_{\text{sources}}, \quad (\text{B.2})$$

with  $S_{\text{grav}}$  and  $S_{\text{sources}}$  given by equations (2.8) and (2.10).

We plug the metric and  $F_3$  ansatz into this action and integrate over all coordinates except  $\rho$ , drop the overall volume factor, and end up with a one-dimensional action with Lagrangian

$$L = \sum_{i,j} G_{ij}(Y) Y_i' Y_j' - U(Y) \equiv T - U. \quad (\text{B.3})$$

We can express the  $Y_i$  in terms of nine other functions to make  $G_{ij}$  diagonal:

$$Y_1 = e^{2z-6x}, \quad Y_2 = e^{2z+2x}, \quad Y_3 = e^{10y-2z+2l}, \\ Y_4 = e^{2y-2z+2p+2q}, \quad Y_5 = e^{2y-2z+2p-2q}, \quad Y_6 = e^{2y-2z-8p}, \\ Y_7 = a, \quad Y_8 = b, \quad Y_9 = \phi. \quad (\text{B.4})$$

We end up with the following expressions:

$$\begin{aligned}
T &= e^{-l} \left( 5y'^2 - 3x'^2 - 2z'^2 - 5p'^2 - q'^2 - \frac{1}{4} e^{-4q} a'^2 - \frac{N_c^2}{64} e^{\phi+4z-4y-4p} b'^2 - \frac{1}{8} \phi'^2 \right), \\
U &= \frac{1}{8} e^l \left[ e^{8y} \{ e^{-12p} [e^{4q} + e^{-4q} (a^2 - 1)^2 + 2a^2 (1 - e^{10p-2q})^2] - 8e^{-2p} \cosh 2q \} \right. \\
&\quad \left. + \frac{N_c^2}{16} e^{\phi+4z+4y+4p} \left\{ e^{4q} + e^{-4q} \left( a^2 - 2ab + 1 - \frac{N_f}{N_c} \right)^2 + 2(a-b)^2 \right\} + N_c e^{\phi/2+2z+6y-4p} \right].
\end{aligned} \tag{B.5}$$

Note that the  $N_c$  dependence can be absorbed by shifting the dilaton, which we will do from now on. We will also write the ratio of the number of flavor branes to color branes as  $s \equiv N_f/N_c$ . Since  $l$  has no kinetic term, it is a pure gauge degree of freedom reflecting the remaining reparametrization invariance. Varying with respect to  $l$  one can set it to any value.

We want to make connection with the metric ansatz given in equation (2.14) in Einstein frame, *i.e.* one in which

$$\begin{aligned}
Y_1 &= e^{\phi/2} e^{-8x}, & Y_2 &= e^{\phi/2}, & Y_3 &= e^{\phi/2} e^{2k} e^{8x}, \\
Y_4 &= e^{\phi/2} e^{2h}, & Y_5 &= (e^{\phi/2} e^{2g})/4, & Y_6 &= (e^{\phi/2} e^{2k})/4, \\
Y_7 &= a, & Y_8 &= b, & Y_9 &= \phi.
\end{aligned} \tag{B.6}$$

In order to do this, we must pick the gauge  $l = -4p - 4y + 4x + \log 2$ , and also make the transformations

$$\begin{aligned}
y &= \frac{1}{10} (4g + 4h + 2k - 10x + 5\phi - 3 \log 4), & p &= \frac{1}{10} (g + h - 2k + \log 2), \\
q &= \frac{1}{2} (-g + h + \log 2), & z &= \frac{1}{4} (-4x + \phi)
\end{aligned} \tag{B.7}$$

After these transformations, the metric ansatz takes the desired form. In practice, we first compute the equations of motion from the Lagrangian in the  $p, q, y, z, l, x, \phi$  variables, and then apply the above transformations to get equations of motion in the  $k, g, h, x, \phi$  variables. This results in equations (2.18 - 2.25) for the EOMs and constraint, given in section 2.2.

We note that the equations of motion and constraint are invariant under constant shifts of the dilaton

$$\Phi \rightarrow \Phi + C, \tag{B.8}$$

as well as shifts in the radial coordinate

$$r \rightarrow r + r_0. \tag{B.9}$$

## C Appendix: UV asymptotics

### C.1 Finite temperature UV asymptotics

In the UV, we express the metric and gauge functions as a series in powers of  $e^{-2\rho/3}$ :

$$\begin{aligned}
e^{2h} &= \sum_{i=0}^{\infty} \sum_{j=0}^i h_{i,j} \rho^j e^{4(1-i)\rho/3} & e^{4\phi} &= \sum_{i=1}^{\infty} \sum_{j=0}^i f_{i,j} \rho^j e^{4(1-i)\rho/3} \\
e^{2g} &= \sum_{i=0}^{\infty} \sum_{j=0}^i g_{i,j} \rho^j e^{4(1-i)\rho/3} & e^{8x} &= \sum_{i=1}^{\infty} \sum_{j=0}^i x_{i,j} \rho^j e^{2(1-i)\rho/3} \\
e^{2k} &= \sum_{i=0}^{\infty} \sum_{j=0}^i k_{i,j} \rho^j e^{4(1-i)\rho/3} & a &= \sum_{i=1}^{\infty} \sum_{j=0}^i a_{i,j} \rho^j e^{2(1-i)\rho/3} \\
&& b &= \sum_{i=1}^{\infty} \sum_{j=0}^i b_{i,j} \rho^j e^{2(1-i)\rho/3}. \tag{C.1}
\end{aligned}$$

The coefficients  $h_{i,j}, \dots, b_{i,j}$  are not all free, and inserting these expansions into the EOMs and constraint equation (2.18 - 2.25) allows us to express them in terms of 11 independent coefficients, which we list here along with their order in the expansion:

$$\begin{aligned}
&x_{1,0} \text{ (const)}, \quad x_{5,0} (e^{-8\rho/3}), \quad f_{1,0} \text{ (const)}, \quad f_{3,0} (e^{-8\rho/3}), \\
&a_{2,0} (e^{-2\rho/3}), \quad a_{4,0} (e^{-2\rho}), \quad b_{4,0} (e^{-2\rho}), \\
&k_{0,0} (e^{4\rho/3}), \quad k_{3,0} (e^{-8\rho/3}), \\
&h_{1,0} \text{ (const)}, \quad h_{1,1} (\rho). \tag{C.2}
\end{aligned}$$

Here we present expressions for the remaining non-zero dependent coefficients in the UV expansions, up to  $\mathcal{O}(\text{poly}(\rho) \times e^{-10\rho/3})$ . In order to simplify some of the higher order coefficients in what follows, we will assume that  $x_{1,0} = 1$  and  $a_{2,0} = 0$ .<sup>11</sup>

•  $\mathcal{O}(e^{4\rho/3})$ :

$$h_{0,0} = \frac{3}{8}k_{0,0} \quad g_{0,0} = \frac{3}{2}k_{0,0} \tag{C.3}$$

•  $\mathcal{O}(\text{const})$ :

$$k_{1,0} = \frac{s}{2}, \quad g_{1,0} = \frac{9s}{4} - 4h_{1,0}, \quad g_{1,1} = -4h_{1,1}, \tag{C.4}$$

---

<sup>11</sup>The latter condition is required for a supersymmetric solution, and we set it equal to zero also in our finite temperature solutions, such that  $C_2$  is the only parameter deforming the BPS backgrounds.

• $\mathcal{O}(e^{-4\rho/3})$ :

$$\begin{aligned}
k_{2,0} &= \frac{1}{36k_{0,0}} \left( 9 + 9s^2 - 256h_{1,0}^2 + 9s(-1 + 16h_{1,0} - 9h_{1,1}) \right. \\
&\quad \left. + 288h_{1,0}h_{1,1} - 216h_{1,1}^2 - \frac{9f_{3,0}k_{0,0}^2}{f_{1,0}} \right) \\
k_{2,1} &= \frac{3(-2+s)^2 + 8(9s - 32h_{1,0})h_{1,1} + 144h_{1,1}^2}{18k_{0,0}} \\
k_{2,2} &= -\frac{64h_{1,1}^2}{9k_{0,0}} \\
g_{2,0} &= \frac{1}{24k_{0,0}} \left( -3 + 60s^2 + 256h_{1,0}^2 - 3s(11 + 48h_{1,0} - 33h_{1,1}) \right. \\
&\quad \left. - 96h_{1,0}h_{1,1} + 120h_{1,1}^2 - \frac{9f_{3,0}k_{0,0}^2}{f_{1,0}} \right) \\
g_{2,1} &= \frac{3(-2+s)^2 + 8(-9s + 32h_{1,0})h_{1,1} - 48h_{1,1}^2}{12k_{0,0}} \quad g_{2,2} = \frac{32h_{1,1}^2}{3k_{0,0}} \\
h_{2,0} &= \frac{1}{96k_{0,0}} \left( -3 + 24s^2 + 256h_{1,0}^2 - 96h_{1,0}h_{1,1} + 120h_{1,1}^2 \right. \\
&\quad \left. - 3s(-13 + 48h_{1,0} + 15h_{1,1}) - \frac{9f_{3,0}k_{0,0}^2}{f_{1,0}} \right) \\
h_{2,1} &= \frac{3(-2+s)^2 + 8(-9s + 32h_{1,0})h_{1,1} - 48h_{1,1}^2}{48k_{0,0}} \\
h_{2,2} &= \frac{8h_{1,1}^2}{3k_{0,0}} \quad f_{2,0} = -\frac{2sf_{1,0}}{k_{0,0}} \tag{C.5}
\end{aligned}$$

• $\mathcal{O}(e^{-2\rho})$ :

$$b_{4,1} = (2-s)a_{4,0} \tag{C.6}$$

• $\mathcal{O}(e^{-8\rho/3})$ :

$$\begin{aligned}
k_{3,1} &= \frac{1}{432f_{1,0}k_{0,0}^2} \left[ sf_{1,0} \left[ 103s^2 - 4s(-125 + 352h_{1,0} + 304h_{1,1}) \right. \right. \\
&\quad \left. \left. + 4 \left( 1 + 1024h_{1,0}^2 + 64h_{1,0}(-7 + 25h_{1,1}) + 4h_{1,1}(-73 + 91h_{1,1}) \right) \right] \right. \\
&\quad \left. + 24s(x_{5,0}f_{1,0} - f_{3,0})k_{0,0}^2 + 576f_{1,0}k_{0,0}^3a_{4,0}^2 \right]
\end{aligned}$$

$$\begin{aligned}
k_{3,2} &= \frac{s \left[ (-2+s)^2 - 8(14+11s-64h_{1,0})h_{1,1} + 400h_{1,1}^2 \right]}{54k_{0,0}^2} \\
k_{3,3} &= \frac{256sh_{1,1}^2}{81k_{0,0}^2} \\
g_{3,0} &= -x_{5,0}h_{1,0} + \frac{f_{3,0}h_{1,0}}{f_{1,0}} + \frac{3}{4}x_{5,0}h_{1,1} + s^2 \left( -\frac{313}{192k_{0,0}^2} - \frac{5h_{1,0}}{3k_{0,0}^2} + \frac{373h_{1,1}}{96k_{0,0}^2} \right) \\
&\quad + s \left( \frac{5}{8}x_{5,0} - \frac{f_{3,0}}{2f_{1,0}} + \frac{313}{192k_{0,0}^2} + \frac{2h_{1,0}}{k_{0,0}^2} - \frac{8h_{1,0}^2}{3k_{0,0}^2} - \frac{79h_{1,1}}{48k_{0,0}^2} - \frac{35h_{1,0}h_{1,1}}{3k_{0,0}^2} - \frac{131h_{1,1}^2}{48k_{0,0}^2} \right) \\
&\quad + \frac{1225s^3}{768k_{0,0}^2} - \frac{7h_{1,0}}{3k_{0,0}^2} - \frac{7h_{1,1}}{4k_{0,0}^2} + \frac{32h_{1,0}^2h_{1,1}}{3k_{0,0}^2} + \frac{40h_{1,0}h_{1,1}^2}{3k_{0,0}^2} + \frac{7h_{1,1}^3}{k_{0,0}^2} - \frac{3}{4}k_{3,0} + \frac{3}{8}k_{0,0}a_{4,0}^2 \\
g_{3,1} &= -x_{5,0}h_{1,1} + \frac{f_{3,0}h_{1,1}}{f_{1,0}} + s^2 \left( -\frac{317}{144k_{0,0}^2} + \frac{16h_{1,0}}{9k_{0,0}^2} + \frac{4h_{1,1}}{9k_{0,0}^2} \right) \\
&\quad + s \left( -\frac{1}{24}x_{5,0} + \frac{f_{3,0}}{24f_{1,0}} + \frac{191}{144k_{0,0}^2} + \frac{52h_{1,0}}{9k_{0,0}^2} - \frac{64h_{1,0}^2}{9k_{0,0}^2} + \frac{145h_{1,1}}{36k_{0,0}^2} \right. \\
&\quad \left. - \frac{148h_{1,0}h_{1,1}}{9k_{0,0}^2} - \frac{511h_{1,1}^2}{36k_{0,0}^2} \right) \\
&\quad + \frac{89s^3}{576k_{0,0}^2} - \frac{8h_{1,0}}{3k_{0,0}^2} - \frac{7h_{1,1}}{3k_{0,0}^2} + \frac{64h_{1,0}h_{1,1}^2}{3k_{0,0}^2} + \frac{40h_{1,1}^3}{3k_{0,0}^2} - k_{0,0}a_{4,0}^2 \\
g_{3,2} &= s^2 \left( \frac{1}{18k_{0,0}^2} + \frac{5h_{1,1}}{9k_{0,0}^2} \right) + s \left( -\frac{1}{18k_{0,0}^2} + \frac{38h_{1,1}}{9k_{0,0}^2} - \frac{64h_{1,0}h_{1,1}}{9k_{0,0}^2} - \frac{74h_{1,1}^2}{9k_{0,0}^2} \right) \\
&\quad - \frac{s^3}{72k_{0,0}^2} - \frac{8h_{1,1}}{3k_{0,0}^2} + \frac{32h_{1,1}^3}{3k_{0,0}^2} \\
g_{3,3} &= -\frac{64sh_{1,1}^2}{27k_{0,0}^2} \\
h_{3,0} &= \frac{1}{4}x_{5,0}h_{1,0} - \frac{f_{3,0}h_{1,0}}{4f_{1,0}} - \frac{3}{16}x_{5,0}h_{1,1} + s^2 \left( -\frac{25}{768k_{0,0}^2} + \frac{5h_{1,0}}{4k_{0,0}^2} + \frac{259h_{1,1}}{384k_{0,0}^2} \right) \\
&\quad + s \left( \frac{1}{64}x_{5,0} + \frac{f_{3,0}}{64f_{1,0}} + \frac{61}{768k_{0,0}^2} - \frac{2h_{1,0}}{3k_{0,0}^2} - \frac{2h_{1,0}^2}{3k_{0,0}^2} - \frac{247h_{1,1}}{192k_{0,0}^2} + \frac{h_{1,0}h_{1,1}}{12k_{0,0}^2} + \frac{229h_{1,1}^2}{192k_{0,0}^2} \right) \\
&\quad - \frac{287s^3}{3072k_{0,0}^2} + \frac{7h_{1,0}}{12k_{0,0}^2} + \frac{7h_{1,1}}{16k_{0,0}^2} - \frac{8h_{1,0}^2h_{1,1}}{3k_{0,0}^2} - \frac{10h_{1,0}h_{1,1}^2}{3k_{0,0}^2} - \frac{7h_{1,1}^3}{4k_{0,0}^2} \\
&\quad - \frac{3}{16}k_{3,0} - \frac{9}{32}k_{0,0}a_{4,0}^2
\end{aligned}$$

$$\begin{aligned}
h_{3,1} &= \frac{1}{4}x_{5,0}h_{1,1} - \frac{f_{3,0}h_{1,1}}{4f_{1,0}} + s^2 \left( -\frac{101}{576k_{0,0}^2} + \frac{7h_{1,0}}{9k_{0,0}^2} + \frac{16h_{1,1}}{9k_{0,0}^2} \right) \\
&+ s \left( -\frac{1}{96}x_{5,0} + \frac{f_{3,0}}{96f_{1,0}} - \frac{25}{576k_{0,0}^2} + \frac{h_{1,0}}{9k_{0,0}^2} - \frac{16h_{1,0}^2}{9k_{0,0}^2} \right. \\
&\quad \left. - \frac{23h_{1,1}}{144k_{0,0}^2} - \frac{37h_{1,0}h_{1,1}}{9k_{0,0}^2} - \frac{79h_{1,1}^2}{144k_{0,0}^2} \right) \\
&- \frac{127s^3}{2304k_{0,0}^2} + \frac{2h_{1,0}}{3k_{0,0}^2} + \frac{7h_{1,1}}{12k_{0,0}^2} - \frac{16h_{1,0}h_{1,1}^2}{3k_{0,0}^2} - \frac{10h_{1,1}^3}{3k_{0,0}^2} - \frac{1}{4}k_{0,0}a_{4,0}^2 \\
h_{3,2} &= s^2 \left( \frac{1}{72k_{0,0}^2} + \frac{17h_{1,1}}{36k_{0,0}^2} \right) + s \left( -\frac{1}{72k_{0,0}^2} - \frac{5h_{1,1}}{18k_{0,0}^2} - \frac{16h_{1,0}h_{1,1}}{9k_{0,0}^2} - \frac{37h_{1,1}^2}{18k_{0,0}^2} \right) \\
&- \frac{s^3}{288k_{0,0}^2} + \frac{2h_{1,1}}{3k_{0,0}^2} - \frac{8h_{1,1}^3}{3k_{0,0}^2} \\
h_{3,3} &= -\frac{16sh_{1,1}^2}{27k_{0,0}^2} \quad f_{3,1} = -\frac{8f_{1,0}}{3k_{0,0}^2} + \frac{8sf_{1,0}}{3k_{0,0}^2} - \frac{2s^2f_{1,0}}{3k_{0,0}^2}
\end{aligned} \tag{C.7}$$

•  $\mathcal{O}(e^{-10\rho/3})$ :

$$\begin{aligned}
a_{6,0} &= -\frac{3sa_{4,0}}{4k_{0,0}} + \frac{8h_{1,0}a_{4,0}}{3k_{0,0}} \quad a_{6,1} = \frac{8h_{1,1}a_{4,0}}{3k_{0,0}} \\
b_{6,0} &= \frac{3s^2a_{4,0}}{128k_{0,0}} + s \left( \frac{3b_{4,0}}{8k_{0,0}} + \frac{21a_{4,0}}{64k_{0,0}} - \frac{3h_{1,0}a_{4,0}}{2k_{0,0}} - \frac{45h_{1,1}a_{4,0}}{32k_{0,0}} \right) \\
b_{6,1} &= -\frac{3s^2a_{4,0}}{8k_{0,0}} + s \left( \frac{3a_{4,0}}{4k_{0,0}} - \frac{3h_{1,1}a_{4,0}}{2k_{0,0}} \right)
\end{aligned} \tag{C.8}$$

## C.2 Supersymmetric UV asymptotics

Here we summarize the BPS, zero-temperature UV asymptotics (up to  $\mathcal{O}(e^{-4\rho/3})$ ) of the backgrounds corresponding to D5s wrapped on the  $S^2$  of the resolved conifold, with the addition of smeared D5 flavor sources, as described in [20, 28]. These serve as matching conditions for our finite temperature UV asymptotics. In addition, they furnish us with a family of reference backgrounds that are used in the energy calculations of section 5.

The BPS asymptotics are given in terms of the free variables  $Q_0, c_+, c_-, \rho_0$  and  $f_{1,0}$  after performing a UV expansion of *e.g.* equations (3.5) of [20].<sup>12</sup> The finite temperature asymptotics of section 3.1 are a deformation of these BPS asymptotics

<sup>12</sup>In [20], the parameter  $\Phi_0$  is used instead of  $f_{1,0}$ . We remove the  $c_+$  dependence of the asymptotically constant part of the dilaton by setting  $e^{4\Phi_0} = 2f_{1,0}c_+^3/3$ . See equation (B.46) of [20].

with  $\rho_0 = 0$ ,  $Q_0 = -N_c + N_f/2$  and  $f_{1,0} = 1$ . In the energy calculations of section 5, we also set  $\rho_0 = 0$ , but  $Q_0$ ,  $c_+$ ,  $c_-$  and  $f_{1,0}$  are left free to allow for the matching.

What follows, then, is the form of the UV BPS asymptotics with  $\rho_0 = 0$ , but with  $Q_0$ ,  $c_+$ ,  $c_-$  and  $f_{1,0}$  left free.<sup>13</sup>

$$\begin{aligned}
e^{2k} &= \frac{2}{3}c_+e^{4\rho/3} + \frac{s}{2} + \frac{1}{96c_+}e^{-4\rho/3} \left[ -64Q_0^2 - 16(3-4\rho)^2 + 16s(3-4\rho)^2 \right. \\
&\quad \left. + 32Q_0(-2+s)(-3+4\rho) + s^2(-27+96\rho-64\rho^2) \right] \\
e^{2h} &= \frac{1}{4}c_+e^{4\rho/3} + \frac{1}{32}(8Q_0+9s-8(-2+s)\rho) \\
&\quad + \frac{1}{256c_+}e^{-4\rho/3} \left[ 64Q_0^2 + 9(16-16s+3s^2) - 128Q_0(-2+s)\rho + 64(-2+s)^2\rho^2 \right] \\
e^{2g} &= c_+e^{4\rho/3} - Q_0 + \frac{9s}{8} + (-2+s)\rho \\
&\quad + \frac{1}{64c_+}e^{-4\rho/3} \left[ 64Q_0^2 + 9(16-16s+3s^2) - 128Q_0(-2+s)\rho + 64(-2+s)^2\rho^2 \right] \\
e^{4\phi} &= f_{10} - \frac{3e^{-4\rho/3}sf_{10}}{c_+} + \frac{3f_{1,0}}{8c_+^2}e^{-8\rho/3} \left[ 4Q_0(-2+s) + s^2(15-4\rho) - 2(3+8\rho) + 2s(3+8\rho) \right] \\
a &= 2e^{-2\rho} \quad b = e^{-2\rho}(2+2Q_0-s-2(-2+s)\rho)
\end{aligned} \tag{C.9}$$

## D Appendix: General form of $B_2$

In the extremal case [20], the  $SU(3)$  structure fixes the form of  $B_2$ . In our solutions  $B_2$  should reduce to the one in [20] when  $T = 0$ . The following ansatz is compatible with that requirement:

$$B_2 = b_1(\rho)\tilde{\omega}_3 \wedge d\rho + b_2(\rho)e_1 \wedge e_2 + b_3(\rho)e_1 \wedge \tilde{\omega}_2 + b_4(\rho)e_2 \wedge \tilde{\omega}_1 + b_5(\rho)\tilde{\omega}_1 \wedge \tilde{\omega}_2. \tag{D.1}$$

We find it convenient to introduce a new function  $\tilde{b}_2(\rho)$  and parametrize  $b_2$  as,

$$b_2(\rho) = \tilde{b}_2(\rho) + (1-a(\rho)^2)b_5(\rho) \tag{D.2}$$

Therefore,

$$B_2 = b_1(\rho)\tilde{\omega}_3 \wedge d\rho + (\tilde{b}_2(\rho) + (1-a(\rho)^2)b_5(\rho))e_1 \wedge e_2 + b_3(\rho)e_1 \wedge \tilde{\omega}_2 + b_4(\rho)e_2 \wedge \tilde{\omega}_1 + b_5(\rho)\tilde{\omega}_1 \wedge \tilde{\omega}_2. \tag{D.3}$$

---

<sup>13</sup> $c_-$  appears only at  $\mathcal{O}(e^{-8\rho/3})$  and higher in the metric functions, which we omit here for brevity.



With this notation it is easy to show that

$$B_2 = (B_2)_{b_5=0} - d[b_5(\rho)\tilde{\omega}_3] \quad (\text{D.4})$$

Thus,  $b_5$  is really a gauge choice that does not affect the value of  $H_3$ .

From (4.1) we have,

$$H_3 = -e^{-4x} \frac{1}{4} e^{2\phi} *_6 f_3 \quad (\text{D.5})$$

Demanding that  $H_3 = d[B_2]$  results in five equations,

$$\begin{aligned} \cot(\theta)(b_3 - b_4) &= 0 \\ b_3 + ab_5 - \frac{1}{8}e^{2\phi-8x}b' &= 0 \\ 2e^{2\phi-2g+2h} - (-1 + a^2)b_1 + (b_3 + b_4 + 2ab_5)a' - \tilde{b}_2' - b_5'(1 - a^2) &= 0 \\ e^{2\phi}(-a + b) - 2(ab_1 + b_5a' + b_3') &= 0 \\ \frac{1}{8}e^{2\phi+2g-2h}(-1 + s - a^2 + 2ab) + b_1 - b_5' &= 0 \end{aligned} \quad (\text{D.6})$$

Three of them are easily solved by setting,

$$\begin{aligned} b_3 &= b_4 \\ b_4 &= -\frac{1}{8}(8ab_5 - e^{2\phi-8x}b') \\ b_1 &= \frac{1}{8}e^{-2h+2g+2\phi}(1 - s + a^2 - 2ab) + b_5' = 0 \end{aligned} \quad (\text{D.7})$$

we are then left with two equations, one of them is just the equation of motion for  $b(\rho)$ . The other one is a differential equation for  $\tilde{b}_2(\rho)$ ,

$$\begin{aligned} e^{2\phi+4g+8x}(sa^2 - a^4 - 2ab + 2a^3b) + e^{2\phi+2g+2h}a'b' + e^{8x+2\phi}(16e^{4h} - e^{4g}(-1 + s)) \\ - e^{8x+2g+2h}\tilde{b}_2'(\rho) = 0 \end{aligned} \quad (\text{D.8})$$

Note that equations (D.7-D.8) determine  $B_2$  in terms of an arbitrary function  $b_5$  that we have shown is just a gauge choice. In order to make contact with [20] we choose,

$$b_5' = \frac{1}{8}e^{2\phi-2h}(4e^{2h+2k} + e^{2g}(-1 + s - a^2 + 2ab)) \quad (\text{D.9})$$

which gives  $b_1 = \frac{1}{2}e^{2\phi+2k}$ .

## E Appendix: Comments on numerical procedure

The UV-shot solutions of section 3.3 were obtained by using Mathematica’s `NDSolve`, with UV boundary conditions determined by the expansions given in equation (C.1) up to  $\mathcal{O}(e^{-8\rho})$  for  $e^{8x}$ ,  $\mathcal{O}(e^{-26\rho/3})$  for  $a$  and  $b$ ,  $\mathcal{O}(e^{-20\rho/3})$  for  $e^{2k}$ ,  $e^{2g}$  and  $e^{2h}$ , and  $\mathcal{O}(e^{-8\rho})$  for  $e^{4\Phi}$ . Using an expansion taken out to this order, `NDSolve` at `WorkingPrecision` = 70 finds a horizon radius  $\rho_h$  which is fairly independent of the value of  $\rho_\infty$  chosen ( $\sim 1$  part in  $10^{-5}$  as  $\rho_\infty$  is varied from 6 to 9). The constraint equation (2.25) is of order  $10^{-8}$  when evaluated on a typical UV-shot solution, but climbs near the horizon; on the horizon shot solution the constraint is of order  $10^{-14}$  with a maximum of  $\sim 10^{-6}$  at the horizon — see Figs. (26) and (27). The degree to which the constraint equation is violated near the horizon also depends on the size of  $C_2$ . This stems from the fact that many higher order terms in the UV expansion are proportional to  $C_2$ , so any finite order truncation of the UV asymptotics becomes less accurate for larger  $C_2$  values.

When matching our UV-shot solutions to a series expansion near the horizon, we choose to exclude the  $a$  and  $b$  functions, the dilaton, and their derivatives from the mismatch function. The reason for excluding the  $a$  and  $b$  functions is that unlike the metric and dilaton functions — whose UV and horizon shot solutions agree quite well away from the horizon in what `NMinimize` considers the best matched case —  $a$  and  $b$ ’s UV and horizon shot solutions differ over the entire interval in the best matched case, as shown in Fig. (28) (although  $a$  and  $b$  are typically small in magnitude compared to  $x, g, h, k$  and  $\Phi$ ). The UV-shot dilaton also displays divergent behavior near the horizon, and drastically decreases the match’s accuracy if included. Including it in the match also produces a horizon-shot dilaton which stabilizes to a UV value different than  $e^{4\phi}|_{\rho_\infty} \sim 1$ . We remedy this by using the invariance of the EOMs under a constant shift in the dilaton. After the matching is performed, we pick an  $f_0$  that gives a horizon-shot dilaton that agrees with the UV value of  $e^{4\phi}|_{\rho_\infty} \sim 1$ . For the solutions we have found, including  $a$ ,  $b$  and the dilaton allows for the mismatch to be minimized to only  $\sim 10^{-2}$ , and the resulting horizon shot solutions for  $(x, g, h, k, f)$  differ significantly from the UV shot solutions. Excluding  $a$ ,  $b$  and  $\Phi$  from the mismatch function, `NMinimize` is able to reduce the mismatch to  $\sim 10^{-7}$ , and the resulting horizon shot solutions for  $(x, g, h, k, \Phi, a)$  agree very closely with the UV shot solutions. This will still leave us with a horizon-shot  $b$  that tends to exponentially diverging behavior at large  $\rho$ . However,  $b_0$  can be tuned to eliminate this divergence, with negligible effect on the behavior of the other functions  $(x, g, h, k, f)$  — see Fig. (28).

Performing our matching close to the horizon (e.g.  $\epsilon = .15$ ) necessarily involves greater errors in the UV-shot solutions. This shows up as horizon-shot solutions that disagree with the UV-shot solutions near  $\rho_\infty$ . To remedy this, we instead begin by

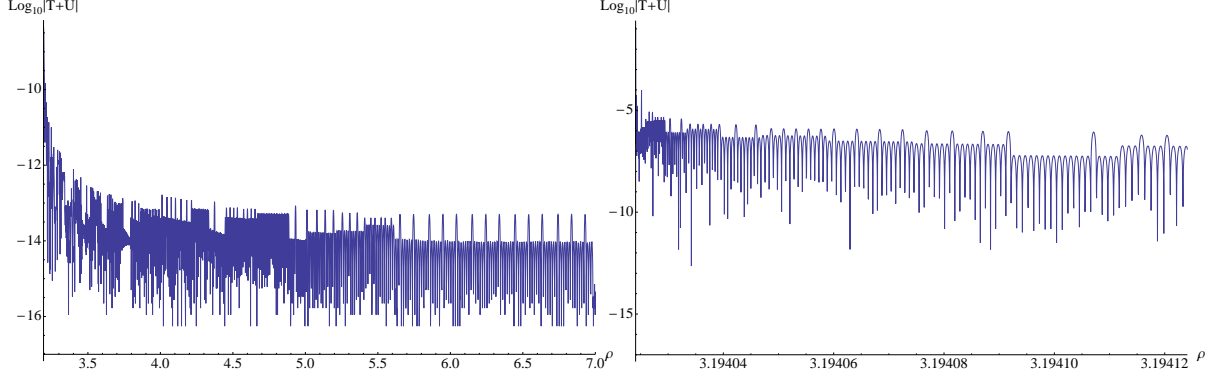


**Figure 26.** Constraint evaluated on a horizon solution, near horizon at  $\rho_h \simeq 3.194024$ . **Figure 27.** Constraint evaluated on same so-shot solution with  $c_+ = 50, C_2 = 5000, s = 1$ .

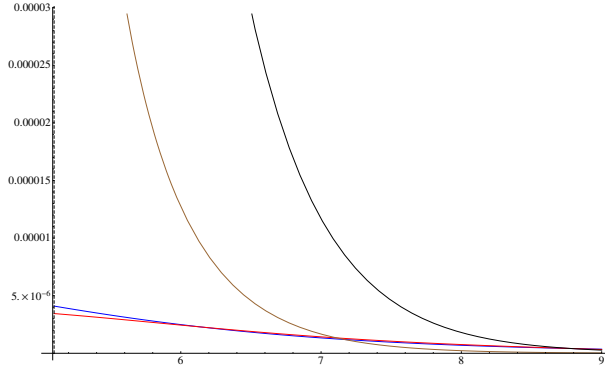


**Figure 28.** Horizon-shot and UV-shot  $a$  and  $b$  after tuning  $b_0$ . brown - UV-shot  $a$ , black - UV-shot  $b$ , blue - horizon shot  $a$ , red - horizon-shot  $b$ .  $s = 1, c = 3, C_2 = 800000$ .

matching at a higher  $\epsilon = .7$  — this eliminates the disagreement near  $\rho_\infty$ . We then use the resulting values of the matched horizon parameters as seeds for a new match performed at a lower  $\epsilon = .15$ , where in addition we constrain the allowed variance of  $(x_1, g_0, h_0, k_0, f_0)$  around the seed values until the resulting  $\epsilon = .15$  match gives horizon shot solutions which agree with the UV shot solutions at  $\rho_\infty$ . After doing this, we find that the high- $\epsilon$ -seeded  $\epsilon = .15$  match produces a mismatch of the same order ( $10^{-7}$ ) as a non-seeded  $\epsilon = .15$  match, with the added benefit that the high- $\epsilon$ -seeded horizon-shot solutions are in good agreement with the UV-shot solutions at  $\rho_\infty$ .

The numerical method we use could undoubtedly be improved. However, as presented here it is enough to identify the behavior of the horizon temperature as a function of the non-extremality parameter  $C_2$ , which is necessary to study the stability of the background. Other methods have been used, such as [18].

## References

- [1] J. M. Maldacena, *The Large  $N$  limit of superconformal field theories and supergravity*, *Adv.Theor.Math.Phys.* **2** (1998) 231–252, [[hep-th/9711200](#)].
- [2] S. Gubser, I. R. Klebanov, and A. M. Polyakov, *Gauge theory correlators from noncritical string theory*, *Phys.Lett.* **B428** (1998) 105–114, [[hep-th/9802109](#)].
- [3] E. Witten, *Anti-de Sitter space and holography*, *Adv.Theor.Math.Phys.* **2** (1998) 253–291, [[hep-th/9802150](#)].
- [4] I. R. Klebanov and M. J. Strassler, *Supergravity and a confining gauge theory: Duality cascades and chi SB resolution of naked singularities*, *JHEP* **0008** (2000) 052, [[hep-th/0007191](#)].
- [5] J. M. Maldacena and C. Nunez, *Towards the large  $N$  limit of pure  $N = 1$  super Yang Mills*, *Phys. Rev. Lett.* **86** (2001) 588–591, [[hep-th/0008001](#)].
- [6] A. Butti, M. Grana, R. Minasian, M. Petrini, and A. Zaffaroni, *The baryonic branch of Klebanov-Strassler solution: A supersymmetric family of  $SU(3)$  structure backgrounds*, *JHEP* **03** (2005) 069, [[hep-th/0412187](#)].
- [7] I. R. Klebanov and J. M. Maldacena, *Superconformal gauge theories and non-critical superstrings*, *Int.J.Mod.Phys.* **A19** (2004) 5003–5016, [[hep-th/0409133](#)].
- [8] F. Bigazzi, R. Casero, A. Cotrone, E. Kiritsis, and A. Paredes, *Non-critical holography and four-dimensional CFT's with fundamentals*, *JHEP* **0510** (2005) 012, [[hep-th/0505140](#)].
- [9] F. Benini, F. Canoura, S. Cremonesi, C. Nunez, and A. V. Ramallo, *Unquenched flavors in the Klebanov-Witten model*, *JHEP* **0702** (2007) 090, [[hep-th/0612118](#)].
- [10] E. Caceres, R. Flauger, M. Ihl, and T. Wrase, *New supergravity backgrounds dual to  $N=1$  SQCD-like theories with  $N(f) = 2N(c)$* , *JHEP* **0803** (2008) 020, [[arXiv:0711.4878](#)].
- [11] F. Bigazzi, A. L. Cotrone, and A. Paredes, *Klebanov-Witten theory with massive dynamical flavors*, *JHEP* **0809** (2008) 048, [[arXiv:0807.0298](#)].
- [12] C. Nunez, A. Paredes, and A. V. Ramallo, *Unquenched Flavor in the Gauge/Gravity Correspondence*, *Adv.High Energy Phys.* **2010** (2010) 196714, [[arXiv:1002.1088](#)].
- [13] F. Benini, F. Canoura, S. Cremonesi, C. Nunez, and A. V. Ramallo, *Backreacting flavors in the Klebanov-Strassler background*, *JHEP* **0709** (2007) 109, [[arXiv:0706.1238](#)].
- [14] F. Bigazzi, A. L. Cotrone, A. Paredes, and A. V. Ramallo, *The Klebanov-Strassler model with massive dynamical flavors*, *JHEP* **0903** (2009) 153, [[arXiv:0812.3399](#)].

- [15] J. Maldacena and D. Martelli, *The Unwarped, resolved, deformed conifold: Fivebranes and the baryonic branch of the Klebanov-Strassler theory*, *JHEP* **1001** (2010) 104, [[arXiv:0906.0591](#)].
- [16] E. Cáceres, C. Nunez, and L. A. Pando-Zayas, *Heating up the Baryonic Branch with U-duality: A Unified picture of conifold black holes*, *JHEP* **1103** (2011) 054, [[arXiv:1101.4123](#)].
- [17] O. Aharony, A. Buchel, and P. Kerner, *The Black hole in the throat: Thermodynamics of strongly coupled cascading gauge theories*, *Phys.Rev.* **D76** (2007) 086005, [[arXiv:0706.1768](#)].
- [18] M. Mahato, L. A. Pando Zayas, and C. A. Terrero-Escalante, *Black Holes in Cascading Theories: Confinement/Deconfinement Transition and other Thermal Properties*, *JHEP* **0709** (2007) 083, [[arXiv:0707.2737](#)].
- [19] A. Buchel, *Chiral symmetry breaking in cascading gauge theory plasma*, *Nucl.Phys.* **B847** (2011) 297–324, [[arXiv:1012.2404](#)].
- [20] J. Gaillard, D. Martelli, C. Nunez, and I. Papadimitriou, *The warped, resolved, deformed conifold gets flavoured*, *Nucl. Phys.* **B843** (2011) 1–45, [[arXiv:1004.4638](#)].
- [21] E. Conde, J. Gaillard, C. Nunez, M. Piai, and A. V. Ramallo, *A Tale of Two Cascades: Higgsing and Seiberg-Duality Cascades from type IIB String Theory*, *JHEP* **1202** (2012) 145, [[arXiv:1112.3350](#)].
- [22] E. Conde, J. Gaillard, C. Nunez, M. Piai, and A. V. Ramallo, *Towards the String Dual of Tumbling and Cascading Gauge Theories*, *Phys.Lett.* **B709** (2012) 385–389, [[arXiv:1112.3346](#)]. 7 pages, 6 figures / v2. minor changes included.
- [23] D. Elander, J. Gaillard, C. Nunez, and M. Piai, *Towards multi-scale dynamics on the baryonic branch of Klebanov-Strassler*, *JHEP* **1107** (2011) 056, [[arXiv:1104.3963](#)].
- [24] E. Cáceres, R. Flauger, and T. Wrase, *Hagedorn Systems from Backreacted Finite Temperature  $N(f)=2N(c)$  Backgrounds*, [[arXiv:0908.4483](#)].
- [25] R. Casero, C. Nunez, and A. Paredes, *Towards the string dual of  $N=1$  SQCD-like theories*, *Phys.Rev.* **D73** (2006) 086005, [[hep-th/0602027](#)].
- [26] S. S. Gubser, *Curvature singularities: The Good, the bad, and the naked*, *Adv.Theor.Math.Phys.* **4** (2000) 679–745, [[hep-th/0002160](#)].
- [27] C. Nunez, A. Paredes, and A. V. Ramallo, *Flavoring the gravity dual of  $N=1$  Yang-Mills with probes*, *JHEP* **0312** (2003) 024, [[hep-th/0311201](#)].
- [28] C. Hoyos-Badajoz, C. Nunez, and I. Papadimitriou, *Comments on the String dual to  $N=1$  SQCD*, *Phys.Rev.* **D78** (2008) 086005, [[arXiv:0807.3039](#)].

- [29] R. Casero, C. Nunez, and A. Paredes, *Elaborations on the String Dual to  $N=1$  SQCD*, *Phys.Rev.* **D77** (2008) 046003, [[arXiv:0709.3421](#)].
- [30] L. A. Pando Zayas and C. A. Terrero-Escalante, *Black holes with varying flux: A Numerical approach*, *JHEP* **0609** (2006) 051, [[hep-th/0605170](#)].
- [31] S. S. Gubser, A. A. Tseytlin, and M. S. Volkov, *NonAbelian 4-d black holes, wrapped five-branes, and their dual descriptions*, *JHEP* **0109** (2001) 017, [[hep-th/0108205](#)].
- [32] J. Gaillard and J. Schmude, *The Lift of type IIA supergravity with D6 sources: M-theory with torsion*, *JHEP* **1002** (2010) 032, [[arXiv:0908.0305](#)].
- [33] S. W. Hawking and G. T. Horowitz, *The Gravitational Hamiltonian, action, entropy and surface terms*, *Class. Quant. Grav.* **13** (1996) 1487–1498, [[gr-qc/9501014](#)].
- [34] A. Cotrone, J. Pons, and P. Talavera, *Notes on a SQCD-like plasma dual and holographic renormalization*, *JHEP* **0711** (2007) 034, [[arXiv:0706.2766](#)].
- [35] A. Buchel, *A Holographic perspective on Gubser-Mitra conjecture*, *Nucl.Phys.* **B731** (2005) 109–124, [[hep-th/0507275](#)].